Electron-spin dephasing via hyperfine interaction in a quantum dot: An equation-of-motion calculation of electron-spin correlation functions

Changxue Deng and Xuedong Hu
Department of Physics, University at Buffalo-SUNY, Buffalo, New York 14260-1500, USA
(Received 25 July 2007; revised manuscript received 30 September 2008; published 2 December 2008)

In this paper we develop an equation-of-motion (EOM) approach to study the *non-Markovian* single-electron-spin dynamics due to its inhomogeneous hyperfine coupling to the surrounding nuclei in a quantum dot. In particular, we identify an electron-spin correlation function that fully represents the electron-spin quantum coherence. Using the EOM method, we recover the exact solution of electron-spin decoherence for the case of a fully polarized nuclear reservoir. By considering nuclear-spin flip-flops mediated by virtual electron flips, which generate fluctuations in the Overhauser field (the nuclear field) for the electron spin, we find that the free-induction decay of the electron-spin correlation function for partially polarized and unpolarized nuclear-spin configurations is of the order unity instead of $O(1/N)$ (N being the number of nuclei in the dot) obtained in previous studies. We show that the complete amplitude decay corresponds to the spectral broadening of the correlation function near the electron-spin Rabi frequency induced by nuclear-spin flip-flops. Our results show that a 90% nuclear-spin polarization can enhance the electron-spin coherence time by more than 1 order of magnitude. In the long-time limit, the envelope of the transverse electron-spin correlation function has a nonexponential $1/t^2$ decay in the presence of both polarized and unpolarized nuclei.

DOI: 10.1103/PhysRevB.78.245301 PACS number(s): 85.35.Be, 76.60.−k, 03.67.Lx

I. INTRODUCTION

Electron-spin dynamics and coherence in semiconductor nanostructures are presently of particular interest both experimentally[1–14] and theoretically,[15–36] because localized electron spins are promising candidates for qubits in spin-based quantum computers.[37,38] Among the many roadblocks to realize such a solid-state quantum computer, controlling the coherent dynamics of the electron spin and maintaining its quantum coherence are of crucial importance.

An electron spin in a semiconductor quantum dot (QD) experiences a variety of interactions, such as spin-orbit coupling and hyperfine coupling.[38] Electron-spin relaxation induced by spin-orbit interaction is quite slow in QDs because of the level discretization.[21] Thus the key system-reservoir interaction for a confined electron in a QD is the hyperfine coupling with the surrounding nuclei. In essence, the nuclear-spin reservoir provides the electron spin a magnetic environment that is random both spatially (due to the fact that nuclear spins are basically thermal, as the relevant experimental temperature of ~100 mK corresponds to the high-temperature limit for the nuclear spins) and temporally (due to nuclear-spin dynamics). The dynamics in the nuclear-spin reservoir is generally what causes electron-spin decoherence.

Nuclear-spin dynamics in a quantum dot is dominated by two types of interactions: the magnetic dipolar interaction between the nuclear spins and the hyperfine interaction between the nuclear and electron spins. Nuclear magnetic dipolar interaction, through direct nuclear-spin flip-flops, gives rise to constant variation in the nuclear-spin configuration, which via the nonuniform hyperfine coupling leads to random fluctuations in the Overhauser field experienced by the electron. The random fluctuations in the nuclear field in turn lead to electron-spin spectral diffusion and pure dephasing at a time scale of tens of microsecond in GaAs and millisecond in Si.[20,25,28,29,32] Dynamics in the nuclear-spin reservoir can also be driven completely by the hyperfine interaction with the electron spin. At lower total fields nuclear spins can flip flop directly with the electron spin, leading to electron-spin relaxation.[19,22] In a finite magnetic field direct flip-flop between electron and nuclear spins is strongly suppressed because of the large Zeeman energy mismatch. Indeed, it has been shown that electron-spin relaxation due to hyperfine interaction is very slow in a finite field.[22] However, in the presence of a large number of nuclear spins, higher-order processes cannot be neglected. For example, electron-mediated nuclear-spin flip-flop, in which the electron spin is only virtually flipped, is not limited by the energy conservation consideration and could be quite important. This effective nuclear-spin interaction works in a similar fashion as the dipolar interaction. It leads to fluctuations in the Overhauser field and thus pure dephasing in the electron spin. Since generally the nuclear dipolar coupling is weaker than the hyperfine interaction in a semiconductor QD, it is important to compare these electron-spin decoherence mechanisms.

The electron-spin decoherence via hyperfine coupling can also be understood from another perspective. A confined electron in a gated quantum dot generally has a nonuniform envelope wave function and a relatively large radius, which leads to an inhomogeneous hyperfine coupling with the nuclear spins on the crystal lattice. The effective number N of nuclear spins involved ranges between 10^3 and 10^6 depending on the actual size of the quantum dot. It is this nonuniformity that causes both electron-spin relaxation and dephasing. Physically this is because the electron acquires a different phase factor each time it interacts with a particular nuclear spin with random orientation. This dephasing effect is dynamical, completely quantum mechanical, and applicable to a single electron spin, in contrast to the dephasing effect caused by inhomogeneous broadening in an ensemble average (represented by a dephasing time T_2^*).[17]

In the context of solid-state quantum information processing, the role of hyperfine interaction could be both positive and negative, depending on the actual experimental objectives. On the one hand, a nuclear-spin bath could be a major decoherence channel for the electron spin that acts as a qubit.[26,37,38] This problem is particularly unavoidable in a GaAs quantum dot, where all the isotopes of Ga and As have nuclear spin $I=\frac{3}{2}$. For a silicon quantum dot this is less of a problem, where the only nuclei of finite spin are ^{29}Si ($I=\frac{1}{2}$, with a natural abundance of 4.68%) and could be removed through isotopic purification. The purified silicon is then made up of only ^{28}Si or ^{30}Si, both having nuclear spin $I=0$. On the other hand, electron-nuclei hyperfine interaction could also be used to control the nuclear spins, which as an ensemble could act coherently. For example it has been suggested that an ensemble of nuclear spins in a quantum dot may be used as a long-lived quantum memory for electron-spin states by transferring the electron-spin state via the hyperfine interaction to nuclear-spin reservoir coherently.[39,40]

The ordinary approach in studying qubit decoherence is to separate the whole system into two parts: the qubit, and the rest of the degrees of freedom as the environment. The qubit-environment coupling should be relatively weak so that it is possible to treat the qubit as a mostly quantum coherent object. In such studies, the Markovian approximation is often used, in which the dynamics within the environment is considered to be so fast that any information transferred from the qubit to the environment is quickly lost without hope of recovery.[41] The problem can then be studied using master equations for the qubit density operator.[41] However, this is not the case for the coupled electron-nuclear-spin system. While nuclear spins form the reservoir here, their dynamics is generally much slower than that of the electron or the coupled dynamics due to hyperfine coupling. The resulting coupled electron-nuclear-spin dynamics is thus non-Markovian and could lead to interesting phenomena such as quantum revival.

The study of non-Markovian electron-spin dynamics in the presence of hyperfine interaction is a complicated quantum many-body (electron and nuclei) problem, and has been studied by many researchers.[18–20,22–30,32–36] An exact solution[19] has been found for an electron interacting with a fully polarized nuclear reservoir. Various types of approaches, such as perturbation theory,[22] pair-correlation approximation,[28] cluster expansion,[29,33,36] equation of motion,[27] and numerical method,[18,23,24,30] have been employed in dealing with this coupled dynamics and the resulting electron-spin decoherence. Numerical studies,[18,23,24,30] limited by the exponentially large Hilbert space, can only be applied to small systems, typically of up to 20 spins.

We have developed an equation-of-motion (EOM) method to study the coupled dynamics of electron and nuclear spins, starting from the exact Hamiltonian for the whole system.[27] We use a systematic large-field expansion method to simplify the equations dramatically, which allows us to solve the full quantum mechanical problem analytically using well-controlled approximations. Within this approach we can obtain a quite complete picture of the electron-spin dynamics in the presence of a large nuclear-spin reservoir. It is important to note that electron-mediated nuclear-spin interactions have been studied for a long time, in both metals and semiconductors.[42–44] For example, conduction-electron-mediated nuclear-spin interaction [Ruderman-Kittel-Kasuya-Yoshida (RKKY)] was discovered in the 1950s and has been studied in various solid-state systems. The difference in our study is that our focus is on a single-electron-mediated RKKY interaction between nuclear spins in a quantum dot, and we are particularly interested in the backaction of this effective nuclear-spin interaction on the *single* mediating electron spin.

Higher-order processes between electron and nuclear spins can in general be classified into two categories, one involving electron-spin flip and the other without electron-spin flip. In a high effective field (external field plus nuclear field), these two types of processes have different consequences. The first type of processes produces longitudinal electron-spin relaxation. However, such real electron-spin flip is energetically unfavorable since the nuclear Zeeman energy is much smaller than that for the electron. Thus this class of processes can be neglected at higher fields. Not surprisingly, a negligible decay amplitude of order $O(\frac{1}{N})$ (N is the number of nuclei involved) for both diagonal (relaxation) and nondiagonal (dephasing) components of the density matrix element of electron spin was found from these processes.[19,22] The second category of processes involves no extra energy transfer since there is no real electron-spin flip between the initial and the final states. Numerical simulations[24] and analytical studies[27,28] have clearly indicated that this kind of processes can contribute significantly to the dephasing of the electron spin, because they cause nuclear-spin configuration variation and thus fluctuations in the Overhauser field. Notice that in the current study we focus on the electron-nuclear-spin dynamics and the resulting electron-spin decoherence in the absence of possible correctional measures such as spin echoes.[43,44] Thus in essence we study the free-induction decay for the electron spin.[43,44] Throughout this paper the words "decoherence" and "dephasing" refer to the loss of quantum coherence of the electron spin during free evolution.

In general, exact solutions cannot be found for nonquadratic Hamiltonians. In terms of the equations of motion, this means that there is an infinite hierarchy of equations when one attempts to evaluate a correlation function. In such cases a decoupling scheme needs to be applied to cut off the series of equations and close the equation set. In the usual many-body treatment, this amounts to calculating some *thermal averages* using the spectral functions determined from the Green's functions self-consistently. However, such approximations involving ensemble averages are not available in the present case, since we are interested in the *real time* dynamics including the coherent part and the decaying part of a single quantum many-body system. In our study we assume that the effective magnetic field (denoting the total of external and nuclear fields) is large so that the electron Zeeman energy is much larger than the single nuclear-spin Zeeman energy, and the direct electron-nuclear-spin flip-flop is suppressed. This assumption greatly simplifies our discussions by selecting one group of equations and correlation functions that describe the main contribution to electron-spin dephasing. Typically, an effective field larger than the fully polar-

ized nuclear field is enough for obtaining self-consistent results. Here we present a detailed exposition of our extensive studies that was discussed only concisely in our Rapid Communication.[27] Below we give a roadmap to the subsequent sections in this paper.

In Sec. II, we lay the foundation of our approach by constructing the Green's function that represents the electron-spin decoherence, including both pure dephasing and relaxation. We then set up the equations of motion for this correlation function, and outline our approach to solve this set of equations by performing a Fourier transform and using proper approximations to cut off the set of algebraic equations of motion so that we can obtain the spectral function of the electron spin, which in turn allows us to calculate the correlation function in the time domain.

In Sec. III we calculate the Green's functions for several different nuclear polarizations of the nuclear-spin reservoir. Specifically, in Sec. III A we use our approach to obtain the exact solution in the case of a fully polarized nuclear reservoir, and verify that our solution is identical to what was obtained before using a different approach. (In Appendix A we also show that the problem of a fully polarized reservoir can be mapped exactly to the noninteracting Anderson model using the Jordan-Wigner representation, so that the exact solution can be obtained accordingly.) In Sec. III B, we analyze a nuclear reservoir that is fully polarized except for one flipped spin. By solving for the correlation function and by inspecting the unitary dynamics of the electron spin we show that the one-spin-flipped reservoir case introduces a dynamical process of electron-mediated nuclear-spin flip-flop, which is absent in the case of a fully polarized reservoir. Furthermore, the one-spin-flipped reservoir represents a very simple context, which allows us to exclusively focus on this dynamical process, showing for example that it should lead to electron-spin decoherence. Notice that the approach we take in this section is independent from the approach we use for Sec. III C because we cannot perform statistical averages for this very special reservoir. As such the validity and justifications of the results of this section should be judged independently from the previous and following sections. In Sec. III C we examine in detail the electron-mediated nuclear-spin flip-flop in the more general situations of unpolarized and partially polarized nuclear reservoirs, focusing on the electron-spin dynamics related to single-pair nuclear-spin dynamics by invoking large-N and mean-field approximations. We obtain the electron-spin spectral functions and the decay behaviors of the electron-spin correlation functions at large time. In Secs. IV and V we discuss the physical meanings of our results and draw our conclusions.

II. METHOD

In this study we focus on the coupled electron-nuclear-spin dynamics in a III-V-type of semiconductor material system such as GaAs. In such direct gap semiconductors the wave function of an electron confined in a quantum dot is mostly dominated by the Bloch function at the Γ point, where the state is made of atomic S orbitals. Therefore the anisotropic part of the hyperfine interaction[34,43] in these systems should be small, and the hyperfine interaction between nuclei and electrons is simply the contact hyperfine interaction described by a simple Hamiltonian,[43,44]

$$H = \omega_0 S^z + \sum_k A_k I_k^z S^z + \sum_k \frac{A_k}{2}(I_k^- S^+ + I_k^+ S^-). \tag{1}$$

Here the first term is the Zeeman energy of the electron spin with $\omega_0 = g^* \mu_B B_0$; the second and third terms are the hyperfine interaction between the electron spin and the nuclear spins. Between the two, the second term represents the nuclear Overhauser field on the electron (quantization axis is already fixed by the external field along the z direction), while the third (last) term describes the flip-flop between the electron and nuclear spins. The Zeeman energies of nuclear spins are neglected, because the Hamiltonian in Eq. (1) conserves the total spin angular momentum, and a single nuclear-spin Zeeman energy is much less than that of the electron spin at a finite magnetic field. Here A_k is the hyperfine coupling constant at the kth nucleus. It is proportional to the probability of the electron at position $\mathbf{r}_k$ and may be written as

$$A_k = A|\psi(\mathbf{r}_k)|^2, \tag{2}$$

where $\psi(\mathbf{r})$ is the electron envelope wave function in the quantum dot (with the complete electron wave function being a product of this envelope function and the underlying Γ-point Bloch wave function at the site of the nuclear spins). A is the total coupling strength between the electron and the nuclei: $\int A(\mathbf{r})d\mathbf{r} = A$. It is determined by the Γ-point Bloch function of the conduction band of the particular material of concern. In a GaAs quantum dot, $A \approx 90$ μeV.[45] For the single-electron wave function, we choose a simple cylindrical form for the quasi-two-dimensional quantum dot, where along the growth direction the wave function is uniform while in the radial direction it is Gaussian:

$$\psi(\rho, z) = \frac{1}{\sqrt{\pi L R}} e^{-\rho^2/2R^2}[\theta(z + L/2) - \theta(z - L/2)].$$

Here $\theta(z)$ is a step function, L is the thickness along the growth direction for the quantum dot, and R is the effective radius of the electron wave function. The effective number of nuclear spins within the quantum dot can then be defined as $N \equiv \pi R^2 L / v_0$, where v_0 is the volume of one unit cell of the host lattice, and we can introduce a unit $A/(Nv_0) \equiv 1$ for the hyperfine interaction strength per unit volume, so that

$$A_k = A(\mathbf{r_k}) = A|\psi(\mathbf{r_k})|^2 = \frac{A}{\pi R^2 L} e^{\rho_k^2/R^2} = \frac{A}{N v_0} e^{\rho_k^2/R^2} = e^{\rho_k^2/R^2}. \tag{3}$$

The total hyperfine interaction strength is now

$$\sum_k A_k = \frac{1}{v_0} \int A(\mathbf{r}) d\mathbf{r} = N.$$

We can conveniently choose v_0 as the unit volume as well, so that energy is measured by A/N while time is measured by N/A ($\hbar = 1$). Consider a reasonably small gated quantum dot with $N = 10^5$, the energy unit is about 1 neV and the time unit

about 1 μs; while for $N=10^6$, the energy unit is about 0.1 neV and the time unit about 10 μs.

The central quantity we calculate is the retarded Green's function of the electron spin

$$G_\perp(t) = -i\theta(t)\langle\Psi_0|S^-(t)S^+(0)|\Psi_0\rangle. \quad (4)$$

Here $\theta(t)$ is the step function and Ψ_0 is the initial wave function of the system (including electron and nuclear spins),

$$|\Psi_0\rangle = [\alpha_0|\Downarrow\rangle + \beta_0|\Uparrow\rangle]|\psi_n\rangle. \quad (5)$$

We assume that the electron and nuclear spins are in a product state at $t=0$, and are therefore not entangled. Furthermore, we assume that initially nuclear spins are in a product state $|\psi_n\rangle=|I_1^z, I_2^z, \ldots, I_k^z, \ldots\rangle$, where $I_k^z=\uparrow$ or $\downarrow$, i.e., nuclear spins could be either up or down at some particular site with a total net nuclear-spin polarization P that will be defined later. For simplicity we assume that the magnitude of the nuclear spins is 1/2 even though $I=3/2$ for all the isotopes of GaAs. This assumption simplifies the algebras in the following study, and we do not anticipate qualitative differences in the properties of $G_\perp(t)$.

It is important to clarify the physical meaning of the Green's function $G_\perp(t)$ defined in Eq. (4). In the high-field limit it is equivalent to the quantum mechanical expectation values of transverse electron-spin operators, $\langle\Psi_0|S^-(t)|\Psi_0\rangle$ or similarly $\langle\Psi_0|S^+(t)|\Psi_0\rangle$, which are important quantities representing the quantum coherence of the electron spin. Substituting Eq. (5) into the expression $\langle\Psi_0|S^-(t)|\Psi_0\rangle$, we find

$$\langle\Psi_0|S^-(t)|\Psi_0\rangle = \alpha_0^*\beta_0\langle\Downarrow,\psi_n|e^{iHt}S^-e^{-iHt}|\Uparrow,\psi_n\rangle + \text{higher-order terms}. \quad (6)$$

Although terms involving real electron-spin flips can also lead to nonzero contributions to the expectation value above, as we have argued in Sec. I and will further illustrate in our calculations below, these terms are of the order $O(1/N)$ for polarized nuclei in the absence of an external magnetic field. The leading-order contribution in Eq. (6) does not involve any real electron-spin flip during the evolution and gives rise to electron-spin pure dephasing (since no energy is transferred between the electron and its environment), while the terms involving electron-spin flip represent relaxation processes involving energy transfer. The leading-order term in Eq. (6) is exactly the Green's function defined in Eq. (4) up to a proportional constant, with the assumption that $|\Psi_0\rangle = |\Downarrow,\psi_n\rangle$.

Another way to understand the pure dephasing term in Eq. (6) is to consider the phase evolution of the electron spin in the Schrödinger picture,

$$G_\perp(t) = -i\theta(t)\langle\Downarrow;\psi_n|e^{iHt/\hbar}S^-e^{-itH/\hbar}S^+|\Downarrow;\psi_n\rangle = -i\theta(t)\{\langle\Downarrow;\psi_n|e^{iHt/\hbar}\}S^-\{e^{-iHt/\hbar}|\Uparrow;\psi_n\rangle\}. \quad (7)$$

The term in the first pair of curly brackets above represents the evolution of the electron-spin-down state in the presence of the hyperfine interaction, while the term in the second pair of curly brackets represents the evolution of the electron-spin-up state in the same environment. If no electron-spin flip occurs, any decay in the calculated average can be attributed solely to dephasing between the electron-spin-up and spin-down states in the same nuclear-spin environment. Obviously, electron-spin flip will also cause decay of this correlation function. Therefore, $G_\perp(t)$ contains the complete decoherence information for the electron spin during its free evolution.

Without loss of generality, we assume $|\Psi_0\rangle=|\Downarrow,\psi_n\rangle$ in the following discussions. The equation of motion for $G_\perp(t)$ takes the form

$$i\frac{d}{dt}G_\perp(t) = \delta(t) - i\theta(t)\langle\Psi_0|[S^-(t),H];S^+(0)|\Psi_0\rangle. \quad (8)$$

The solution of this equation can be obtained in the frequency domain by performing a Fourier transform, after which we have an algebraic equation in the form of the standard equation of motion for the correlation function of two arbitrary operators

$$\omega\langle\langle\hat{A};\hat{B}\rangle\rangle_\omega = \langle\Psi_0|\hat{A}\hat{B}|\Psi_0\rangle|_{t=0} + \langle\langle[\hat{A},H];\hat{B}\rangle\rangle_\omega, \quad (9)$$

where expectation value in the first term on the right-hand side is calculated at the initial time, and $\langle\langle\hat{A};\hat{B}\rangle\rangle_\omega \equiv \int(-i)\theta(t)\langle\Psi_0|\hat{A}(t)\hat{B}(0)|\Psi_0\rangle e^{i\omega t}dt$.

Although the hyperfine Hamiltonian [Eq. (1)] has a simple form, a general analytical solution has not been found. Instead one has to search for approximate solutions under various conditions. Exact solutions can be found in two simple cases: a system with fully polarized initial nuclear-spin configuration,[19] and a Hamiltonian with uniform coupling constants.[19,39]

Here we first set up the equations of motion for the Green's function and the related correlation functions, then either seek analytical solutions in special cases or look for appropriate schemes of cutoff in order to obtain a closed set of equations. By calculating the spin commutators repeatedly, we find the following equations for $G_\perp(\omega)$:

$$(\omega-\Omega_0)G_\perp(\omega) = 1 - \sum_k A_k\langle\langle n_k S^-;S^+\rangle\rangle_\omega - \sum_k A_k\langle\langle I_k^- S^z;S^+\rangle\rangle_\omega,$$

$$\left(\omega^2-\frac{A_k^2}{4}\right)\langle\langle I_k^-;S^+\rangle\rangle_\omega = -\frac{A_k}{2}\left(\omega+\frac{A_k}{2}\right)G_\perp(\omega) + \omega A_k\langle\langle n_k S^-;S^+\rangle\rangle_\omega + \frac{1}{2}\sum_{k'(k)} A_k A_{k'} V_{kk'}(\omega),$$

$$\left(\omega^2-\frac{A_k^2}{4}\right)\langle\langle I_k^- S^z;S^+\rangle\rangle_\omega = \frac{A_k^2}{4}\langle\langle n_k S^-;S^+\rangle\rangle_\omega - \frac{A_k}{4}\left(\omega+\frac{A_k}{2}\right)G_\perp(\omega) + \omega\sum_{k'(k)}\frac{A_{k'}}{2}V_{kk'}(\omega), \quad (10)$$

with

$$V_{kk'}(\omega) = \langle\langle I_k^- S^+ I_{k'}^-; S^+\rangle\rangle_\omega - \langle\langle I_k^- I_{k'}^+ S^-; S^+\rangle\rangle_\omega, \tag{11}$$

where $n_k = \frac{1}{2} - I_k^z$ and $\Omega_0 = \omega_0 + \frac{N}{2}$. Here Ω_0 is the effective magnetic field for a fully polarized nuclear-spin reservoir. $\Sigma_{k'(k)}$ represents the summation over nuclear-spin index k' for $k' \neq k$. After rearranging the equations, we find

$$\begin{aligned}[\omega - \Omega_0 - \Sigma_0(\omega)]G_\perp(\omega) = 1 &- \sum_k A_k \langle\langle n_k S^-; S^+\rangle\rangle_\omega \\ &- \frac{\omega}{2}\sum_{k\neq k'} \frac{A_k A_{k'}}{(\omega^2 - A_k^2/4)} V_{kk'}(\omega) \\ &- \frac{1}{4}\sum_k \frac{A_k^3}{(\omega^2 - A_k^2/4)} \langle\langle n_k S^-; S^+\rangle\rangle_\omega\end{aligned} \tag{12}$$

with the self-energy

$$\Sigma_0(\omega) = \frac{1}{4}\sum_k \frac{A_k^2}{\omega - A_k/2}. \tag{13}$$

The meanings of the various correlations are quite clear. For example, $\langle\langle n_k S^-; S^+\rangle\rangle_\omega$ represents the Fourier transform of the time-correlation function for flipping the electron spin to the down state at time t while the kth nuclear spin is also in the down state ($n_k = 1$). Both $\langle\langle I_k^-; S^+\rangle\rangle_\omega$ and $\langle\langle I_k^- S^z; S^+\rangle\rangle_\omega$ describe the direct electron-nuclear-spin flip-flop. The only difference between them is that the latter depends on the electron-spin state. We will use $\Omega = \omega_0 + \Sigma_k A_k \langle\Psi_0|I_k^z|\Psi_0\rangle$ to represent the total effective magnetic field experienced by the electron (the external field plus the initial nuclear-spin Overhauser field) in the following discussion. $1/\Omega$ will be taken as an important expansion parameter in Sec. III when we look for solutions of Eq. (10). The condition $\Omega \sim N$ corresponds to polarized nuclei and/or external magnetic field above a few Tesla. It is a good starting point for simplifying the EOMs.

After finding $G_\perp(\omega)$, the real time dynamics of the Green's function, $G_\perp(t)$ can be calculated via an inverse Fourier transform,

$$G_\perp(t) = -i\theta(t)\int_{-\infty}^{\infty} \rho(\omega) e^{-i\omega t} d\omega, \tag{14}$$

where the spectral function $\rho(\omega)$ is obtained by analytical continuation ($\omega \to \omega + i0^+$) using $G_\perp(\omega)$ (Ref. 46):

$$\rho(\omega) = -\frac{1}{\pi}\mathrm{Im}\, G_\perp(\omega + i0^+). \tag{15}$$

The imaginary part of the retarded Green's function contains contributions from poles and branch cuts.[46] In our case here the poles determine the renormalized energy of the electron spin, or its precession frequency; while the branch cut describes the decay of the electron-spin state.

It is important to emphasize that while Eq. (10) is exact, it is not closed. There is an infinite hierarchy of equations for increasingly higher-order correlation functions (for example, each of the correlation functions contained in $V_{kk'}(\omega)$ has its own equation of motion that involves higher-order correlation functions). The key in solving this problem is then a controlled cutoff scheme that allows us to extract the most relevant physics in this problem. We use various approximations in calculating the general solution of an arbitrary nuclear polarization with $\Omega \sim N$. One is the large-N expansion, where we neglect A_k when A_k and Ω appear together, since $A_k \sim 1$ and $\Omega \sim N$. This mathematical approximation leads to significant simplifications in our EOMs. We try to explain its physical meaning in any specific situation in more concrete terms in the text. Another is the large-field expansion, which is only used in order to obtain the high-frequency solution for nuclear reservoirs with partially polarized and unpolarized nuclei. It is a physical approximation that allows us to select a group of EOMs that describe the major contributions to the self-energies.

III. SOLUTIONS OF THE GREEN'S FUNCTION

In this section we solve the electron-spin correlation function $G_\perp(\omega)$ defined in Eq. (10) under three different initial nuclear-spin conditions. We first solve the case of a fully polarized nuclear reservoir using the equation-of-motion approach. Next, to illustrate the role of electron-mediated flip-flopping of nuclear spins, we compare our exact solution of the case of fully polarized nuclei, where no indirect nuclear-spin exchange is allowed, with that of the case in which one of the nuclear spins is in the down state initially while all the other nuclear spins point up. Last, we solve the general case of partially polarized or unpolarized nuclear-spin reservoir, focusing on the decohering effect of electron-mediated nuclear-spin flip-flops.

A. Fully polarized nuclear reservoir

The exact solution to the case where an electron spin interacts with a fully polarized reservoir is known.[19] Here we solve this problem within our EOM approach for the sake of completeness and for comparison with other situations. Using the EOMs we have derived, we can obtain the exact solution straightforwardly. One crucial argument we use to simplify the EOMs is the conservation of angular momentum at any time during the evolution. For initially fully polarized nuclei (all nuclear spins in the up state) and initial wave function $\Psi_0 = |\Downarrow, \psi_n\rangle$, this means that at all times there is only one spin (either the electron spin or one of the nuclear spins) in the down state. This restriction eliminates all the higher-order correlation functions present in Eq. (12). For example, $\langle\langle n_k S^-; S^+\rangle\rangle_\omega = 0$ because when the electron spin is flipped down, $n_k = 1/2 - I_k^z$ must be zero for fully polarized nuclei. $V_{kk'}(\omega)$ vanishes for the same reason. Therefore, from Eq. (12) we obtain

$$G_\perp(\omega) = \frac{1}{\omega - \Omega_0 - \Sigma_0(\omega)}, \tag{16}$$

where $\Omega_0 = \omega_0 + N/2$ is the total effective field for an electron in a fully polarized nuclear reservoir. Assuming that the hyperfine coupling constant takes the form of Eq. (3), the real and imaginary parts of the self-energy are

$$\mathrm{Re}\,\Sigma_0(\omega)=\frac{1}{4}\int_0^\infty \frac{A_k^2}{\omega-\frac{A_k}{2}}dk=-\frac{N}{2}-N\omega\ln\left|1-\frac{1}{2\omega}\right|, \tag{17}$$

and

$$\mathrm{Im}\,\Sigma_0(\omega)=-\frac{\pi}{4}\int_0^\infty A_k^2\delta\left(\omega-\frac{A_k}{2}\right)dk = \begin{cases} -N\pi\omega & \text{for } 0<\omega\le\frac{1}{2} \\ 0 & \text{for } \omega\le 0 \text{ or } \omega>\frac{1}{2}. \end{cases} \tag{18}$$

In both calculations we have converted the sum over k into an integral and used the formula

$$\frac{1}{x-a+i0^+}=P\left\{\frac{1}{x-a}\right\}+i\pi\delta(x-a).$$

The imaginary part of the self-energy is nonzero only when $0<\omega\le 1/2$ due to the constraint imposed by the delta function in Eq. (18). The spectral function can be calculated with Eq. (15),

$$\rho(\omega) = \begin{cases} Z_p\delta(\omega-\Omega_0-\mathrm{Re}\,\Sigma_0) & \omega\sim N \\ \frac{1}{N\omega}\dfrac{1}{\left[-\frac{\omega_0}{N\omega}+\frac{1}{N}+\ln\left|1-\frac{1}{2\omega}\right|\right]^2+\pi^2} & 0<\omega<\frac{1}{2}. \end{cases} \tag{19}$$

The renormalization factor Z_p is defined as[46]

$$Z_p=\frac{1}{\left|1-\frac{\partial\Sigma_0(\omega)}{\partial\omega}\right|_{\omega_p}}, \tag{20}$$

where ω_p is the solution to the equation $\omega-\Omega_0-\mathrm{Re}\,\Sigma_0(\omega)=0$. When $\omega_0=0$ (zero external field), $\omega_p\approx N/2+1/4$ and $Z_p\approx 1-1/2N$. It is clear from Eq. (19) that there are two contributions to the spectral function $\rho(\omega)$, namely a pole near Ω and a branch cut in the range of $[0,\frac{1}{2}]$ (shown in the left panel of Fig. 2 schematically). In the fully polarized case, the weight of the pole is close to 1, with only a small fraction of the spectral function in a continuous spectrum. Only the branch cut or continuous spectrum contributes to decoherence, as indicated in the calculation of $G_\perp(t)$ in Eq. (14). Thus electron spin in a fully polarized nuclear environment can maintain the bulk of its quantum coherence for an infinite time.

In Appendix A we show that this exact solution can also be found using the Jordan-Wigner representation, which maps the original spin Hamiltonian into the noninteracting Anderson impurity model.[47] The physical meaning of the exact solution of the Anderson model is that part of the time the electron spin (localized state) is in the spin-down state, and part of the time one of the nuclear spins (continuous state) occupies the down state. The true eigenstates (resonant scattering) are linear combinations of these states.

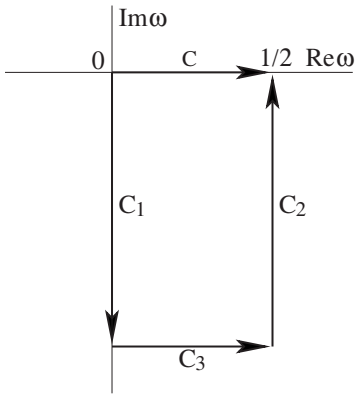

FIG. 1. To obtain the asymptotic behavior of $G_\perp(t)$ at large time, the Fourier integral in Eq. (14) is converted into a Laplace integral by deforming the original contour C into $C_1+C_2+C_3$ as shown above and then allowing $\omega\to\infty$.

In order to obtain the real time spin dynamics we perform an inverse Fourier transform as in Eq. (14). This is straightforward for the delta function part of $\rho(\omega)$, the contribution from the pole. However, the branch cut integration is much more complicated, and we did not find a closed form.

To investigate the long-time decay of the Green's function, we use the method of the steepest descent[48] in numerically evaluating the inverse Fourier transform at the large time limit. The approximate calculation of the integral is performed by deforming the integration contour in the complex ω plane, so that Laplace's method can be used, where the integration of an exponential function is approximated by the integral of this function in the neighborhood of the global maximum of the integrand. Specifically, we deform the original integration contour C into C_1, C_2, and C_3 as shown in Fig. 1. The integration along C_3 at infinity in the lower half plane is exponentially small in the large time limit. This is exactly in the spirit of steepest descent, as one can see the term $e^{-i\omega t}$ is negligible if ω is analytically extended to the complex plane through $\omega=-is$ and s is allowed to approach positive infinity. Substituting the spectral function into Eq. (14) we obtain

$$G_\perp(t)=\left[1+O\left(\frac{1}{N}\right)\right]e^{-iN/2t}+\frac{1}{N}\int_0^{1/2}\frac{1}{\omega}\frac{e^{-i\omega t}d\omega}{\left[\frac{1}{N}+\ln\left|1-\frac{1}{2\omega}\right|\right]^2+\pi^2}, \tag{21}$$

where we have neglected the factor $-i\theta(t)$ in Eq. (14) and assumed that $\omega_0=0$ (no applied field). On the contour C_1 where $\omega=-is$, the integral is determined by the integration interval near $s=0^+$ as $t\to+\infty$ because of the term e^{-st}. By performing a Taylor expansion around $s=0^+$ we obtain $\rho_\perp(-is)=\frac{i}{Ns(\ln s)^2}$. The asymptotic form of the integral for the inverse Fourier transform when $t\to\infty$ is thus

$$G_{\perp}(t)=\left[1+O\left(\frac{1}{N}\right)\right]e^{-iN/2t}+\frac{1}{N}\left[\frac{1}{\ln t}+\left(\ln 2-\ln\gamma+i\frac{\pi}{2}\right)\frac{1}{(\ln t)^2}\right]+O\left[\frac{1}{N}\frac{1}{(\ln t)^3}\right], \tag{22}$$

where $\gamma=-\int_0^\infty \ln s e^{-s}ds$ is the Euler constant. The integral along C_3 has a smaller contribution that is proportional to $\frac{1}{Nt\ln t}$.

The amplitude of the Green's function decays only partially of the order $O(\frac{1}{N})$. Its leading-order time dependence at long time is $1/\ln t$. The oscillatory part takes the form $[1+O(\frac{1}{N})]e^{-iN/2t}$. Our results, obtained with a different method, agree with those found previously.[19]

B. One-spin-flipped nuclear reservoir

The exact solution for the fully polarized nuclear reservoir is a good starting point in our study of hyperfine interaction induced electron-spin decoherence. An important theoretical question now is whether there is any qualitative difference in the spectral function, spin correlation, and its decay when the electron interacts with a partially polarized or unpolarized nuclear reservoir. To find some clues to the answer of this question, we first consider another simple case, where an electron interacts with a nuclear reservoir that has one and only one flipped nuclear spin in an otherwise fully polarized initial nuclear-spin state. In other words, we take the system initial state as

$$|\Psi_0\rangle=|\Downarrow;\uparrow_1,\uparrow_2,\ldots,\downarrow_{\bar{k}},\ldots,\uparrow_N\rangle,$$

where $\bar{k}$ is the index of the initially flipped nuclear spin.

The set of EOMs can be properly closed in this simple case. In Appendix B we give the complete set of EOMs, including all the nonvanishing higher-order correlation functions. Together with Eq. (12), these six equations form a closed set. The even higher-order correlation functions vanish because of conservation of angular momentum, as we have discussed in the case of the fully polarized nuclear reservoir. These equations are obtained from the iterative EOMs by calculating the commutators, and are exact.

For convenience we discuss the low-energy ($|\omega|<\frac{1}{2}$) and high-energy ($\omega\sim\Omega$) solutions of this problem separately. From the exact solution of the fully polarized case, we already know that the spectral function behaves quite differently in these two regimes. There the low-energy part contains a continuous spectrum, while the high-energy part is just a delta function that gives rise to undamped coherent oscillations for the electron spin.

In the following we discuss both the low-energy and high-energy solutions of one-spin-flipped nuclear reservoir with $1/N$ expansion. Since N is very large, this approximation should catch the main physics of the problem.

1. Low-energy solution

As we point out in Sec. I, we assume the existence of a large effective field so that $\Omega\sim N$. In the case of a one-spin-flipped nuclear reservoir, this effective field is $\Omega\approx\Omega_0$, which comes from either the nuclear field alone [Overhauser field from such a nuclear reservoir is $N/2-O(1)$] or in combination with an applied field. Therefore, in the low-energy regime, $\omega\ll\Omega$, in addition to the condition $A_k\ll\Omega$. We can then use the approximation $\omega\pm\Omega\mp\frac{A_k+A_{k'}}{2}\approx\pm\Omega$. In other words, we neglect ω and A_k whenever they appear in a sum with Ω. This amounts to an approximation that helps us find the leading-order solutions.

The right-hand side of Eq. (12) indicates that its solution requires knowledge of $\langle\langle n_k S^-;S^+\rangle\rangle_\omega$ and $V_{kk'}(\omega)$. From Eq. (B1), we obtain

$$\langle\langle n_k S^-;S^+\rangle\rangle_\omega=-\frac{1}{\Omega_0+\Sigma_0(\omega)}\langle n_k\rangle_0+\frac{1}{4[\Omega_0+\Sigma_0(\omega)]}\sum_{k'(k)}\frac{A_kA_{k'}}{\omega+\frac{A_k}{2}}V_{kk'}(\omega)+\frac{1}{4[\Omega_0+\Sigma_0(\omega)]}\sum_{k'(k)}\frac{A_kA_{k'}}{\omega-\frac{A_{k'}}{2}}V_{k'k}(\omega)+O\left(\frac{1}{\Omega^2}\right). \tag{23}$$

Here the self-energy term $\Sigma_0(\omega)$ is of the order $O(N)$ because it involves a summation over nuclear sites of $O(1)$ quantities [also see Eq. (18) for the fully polarized nuclear reservoir]. Equation (10) and the equations in Appendix B indicate that $V_{kk'}(\omega)\sim\langle\langle n_kS^-;S^+\rangle\rangle_\omega$, since $V_{kk'}(\omega)\sim\langle\langle I_k^zS^-;S^+\rangle\rangle_\omega/\Omega$ according to Eq. (B4). Substituting this relation into Eq. (10) then leads to $V_{kk'}(\omega)\sim\langle\langle n_kS^-;S^+\rangle\rangle_\omega$. With these results we can determine the order of magnitude of the summation $\Sigma_kA_k\langle\langle n_kS^-;S^+\rangle\rangle_\omega$ using Eq. (23),

$$\sum_k A_k\langle\langle n_kS^-;S^+\rangle\rangle_\omega\propto\frac{1}{\Omega_0+\Sigma_0(\omega)}\sum_k\langle n_k\rangle_0\propto O\left(\frac{1}{\Omega}\right), \tag{24}$$

since $\Sigma_k\langle n_k\rangle_0=1$. [Recall that there is only one nuclear spin in the down state ($n_{\bar{k}}=1$) initially, and all other nuclear spins point up ($n_k=0$).] Similarly, both the third and the fourth terms on the right-hand side of Eq. (12) are of the order $O(\frac{1}{\Omega})$. Therefore the leading-order low-energy solution of $G_\perp(\omega)$ is

$$G_\perp(\omega)=-\frac{1}{\Omega_0+\Sigma_0(\omega)}+O\left(\frac{1}{\Omega^2}\right), \tag{25}$$

valid for $\omega\sim O(1)$. This solution is identical to the leading-order approximation of the fully polarized nuclear reservoir in the low-energy limit. There are only higher-order differences between the two cases in this regime. The leading-order spectral functions also have the same behavior.

2. High-energy solution

In the high-energy limit, $\omega\sim\Omega$, so that $A_k\ll\omega,\Omega$. Generally we can drop A_k in expressions such as $\omega\pm\frac{A_k}{2}$ and

$\Omega \pm \frac{A_k}{2}$. However, we must use caution when dealing with terms containing $\omega - \Omega \pm \frac{A_k}{2}$. Since both ω and Ω are of order N, the difference between them could be $O(1)$. Thus we can no longer neglect the A_k terms in this type of expressions. Using the large-N expansion again, we find that Eq. (B1) can be simplified to

$$\langle\langle n_k S^-; S^+\rangle\rangle_\omega = \frac{1}{\omega - \Omega_0 - \Sigma_0(\omega) + A_k}\left[\langle n_k\rangle_0 - \frac{A_k}{4\Omega}(f_k + g_k)\right], \tag{26}$$

where $f_k(\omega) = \Sigma_{k'(k)} A_{k'} V_{k'k}(\omega)$ and $g_k(\omega) = \Sigma_{k'(k)} A_{k'} V_{kk'}(\omega)$. Substituting Eq. (26) into Eq. (12), we obtain

$$G_\perp(\omega) = \frac{1}{\omega - \Omega_0 - \Sigma_0(\omega) + A_{\bar{k}}} - \frac{1}{4\Omega}\sum_{k \neq k'} \frac{A_k A_{k'}[V_{kk'}(\omega) + V_{k'k}(\omega)]}{\omega - \Omega_0 - \Sigma_0(\omega) + A_k}. \tag{27}$$

Here $V_{kk'}(\omega)$ contains two terms, one of which is negligible compared to the other in the high-energy limit. It can be shown that $\langle\langle I_k^- S^+ I_{k'}^-; S^+\rangle\rangle_\omega \sim O(\frac{1}{\Omega})\langle\langle I_k^- I_{k'}^+ S^-; S^+\rangle\rangle_\omega$. This relationship is to be expected as $\langle\langle I_k^- S^+ I_{k'}^-; S^+\rangle\rangle_\omega$ corresponds to the electron being flipped during the evolution, which is a low probability event of the order $O(\frac{1}{N})$. We use similar simplifications when searching for solutions of partially polarized and unpolarized nuclei.

In order to evaluate $V_{kk'}(\omega)$, we first use the large-N expansion to simplify Eqs. (B2) and (B5):

$$\langle\langle I_k^- n_{k'}; S^+\rangle\rangle_\omega = -\frac{A_k}{2\Omega}\langle\langle n_{k'} S^-; S^+\rangle\rangle_\omega + \frac{A_{k'}}{2\Omega} V_{kk'}(\omega), \tag{28}$$

and

$$\langle\langle I_k^- I_{k'}^+ I_{k''}^-; S^+\rangle\rangle_\omega = \frac{A_k}{2\Omega} V_{k''k'}(\omega) + \frac{A_{k''}}{2\Omega} V_{kk'}(\omega). \tag{29}$$

Combining Eqs. (B4), (10), (28), and (29), we obtain an implicit equation for $V_{kk'}(\omega)$,

$$\left(\tilde{\omega} + \frac{A_k + A_{k'}}{2}\right) V_{kk'}(\omega) = -\frac{A_k A_{k'}}{4\Omega}\frac{\langle n_k\rangle_0}{\omega - \Omega_0 - \Sigma_0 + A_k} - \frac{A_k A_{k'}}{4\Omega}\frac{\langle n_{k'}\rangle_0}{\omega - \Omega_0 - \Sigma_0 + A_{k'}} + \frac{1}{4\Omega}[A_k f_{k'}(\omega) + A_{k'} g_k(\omega)], \tag{30}$$

where $\tilde{\omega} = \omega - \Omega_0 - \frac{A_2}{4\Omega}$ and $A_2 = \Sigma_k A_k^2$. The hyperfine coupling in Eq. (2) dictates that $A_2 = \frac{N}{2}$. Multiplying both sides of Eq. (30) by $A_{k'}/[\tilde{\omega} + (A_k + A_{k'})/2]$ and summing over k', we arrive at the equation for $f_k(\omega)$,

$$(\Omega - \alpha_k) f_k = -\frac{\alpha_k A_k \langle n_k\rangle_0}{\omega - \Omega_0 - \Sigma_0 + A_k} - \frac{A_k A_{\bar{k}}^2 (1 - \delta_{k\bar{k}})}{4\left(\tilde{\omega} + \frac{A_k + A_{\bar{k}}}{2}\right)(\omega - \Omega_0 - \Sigma_0 + A_{\bar{k}})} + \frac{1}{4}\sum_{k''(k)} \frac{A_k A_{k''}}{\left(\tilde{\omega} + \frac{A_k + A_{k''}}{2}\right)} g_{k''}, \tag{31}$$

where

$$\alpha_k(\tilde{\omega}) = \frac{1}{4}\sum_{k''} \frac{A_{k''}^2}{\tilde{\omega} + \frac{A_k + A_{k''}}{2}}. \tag{32}$$

The equation for g_k is obtained by interchanging f_k and g_k in Eq. (31). The symmetry of the equations for f_k and g_k leads to $f_k = g_k$ in the leading-order large-field (Ω) expansion.

Equation (31) can be transformed to an integral equation, though still difficult to solve. Nevertheless, for our present purpose, Eqs. (27) and (31) are sufficient to further our discussions. First, by solving the equation $\omega - \Omega_0 - \Sigma_0(\omega) + A_{\bar{k}} = 0$, we obtain the same pole (slightly shifted) as the case of fully polarized reservoir. The pole now has a reduced weight as the residue is $Z_p \approx 1 - \frac{1}{2N} - O(1/N)$, where the first two terms come from the first term on the right-hand side of Eq. (27), while the last one $[O(1/N)]$ is a contribution from f_k [the second term on the right-hand side of Eq. (31)]. Since the contribution from f_k is only of order $O(1/N)$, the difference between the present case and the fully polarized nuclear reservoir ($Z_p \approx 1 - 1/2N$ in the exact solution) is very small.

There is one significant qualitative difference between the current solution and that for the fully polarized nuclear reservoir. The function $f_k(\omega)$ has a nonvanishing imaginary part when the frequency ω is in the neighborhood of Ω. In other words, the spectral function has a branch cut contribution near Ω, which leads to decoherence that does not exist in the case of a fully polarized reservoir. This additional contribution to the spectral function is only of the order $O(\frac{1}{N})$ because the δ function in the spectral function has a weight of $1 - O(\frac{1}{N})$ and the total weight of the spectral function is 1. In other words, the new decoherence effect is small, consistent with the fact that the present nuclear reservoir is only different from the fully polarized reservoir by one nuclear-spin flip.

Combining these discussions with the physical picture we have established in the low-frequency region, we summarize the properties of the spectral function in the case of a one-spin-flipped nuclear reservoir in the right panel of Fig. 2 schematically. In the left panel, we draw the schematic of the spectral function of the exact solution in the case of fully polarized reservoir. A comparison of the two panels clearly identifies the difference between the two situations. In the fully polarized case, the only possible process is the electron-nuclei flip-flop (see the upper figure in Fig. 3). The electron flipped state is a high-energy state, by the amount of electron

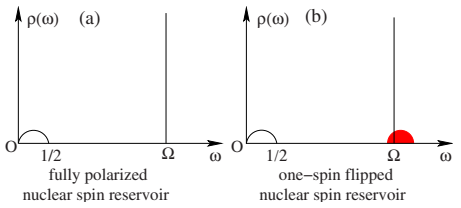

FIG. 2. (Color online) Schematics of the electron-spin spectral function for nuclear reservoirs of fully polarized nuclei (left panel) and one-spin flipped nuclei (right panel). The shaded area in the right figure denotes the contribution of the branch cut by considering electron-mediated nuclear-spin flip-flop that is not possible in the case of fully polarized nuclei. Also the delta function represented by the vertical line has a slightly reduced weight compared to that in the fully polarized case.

Zeeman energy $\hbar\Omega$ (neglecting the nuclear Zeeman energy). For a one-spin-flipped nuclear reservoir, nuclear-spin flip-flop mediated by a virtual electron flip is also possible (see the lower figure in Fig. 3). In the initial and final states, the electron-spin state remains unchanged, but two nuclear spins exchange their states. The virtual (intermediate) state is a high-energy state, and the cross section of this process is proportional to $|1/\Omega|^2$.

An interesting question here is how the δ function in the case of a fully polarized nuclear reservoir evolves into a continuous function in the unpolarized case (as we will show later), with the one-spin-flipped reservoir as the first step of this evolution. What we show here seems to indicate that the δ function might gradually reduce its weight and be replaced by a continuous function. However, the result here needs to be considered within its context: it is obtained with the help of the large-N expansion. The consequence of taking large-N expansion is that the location of the spectral function peak

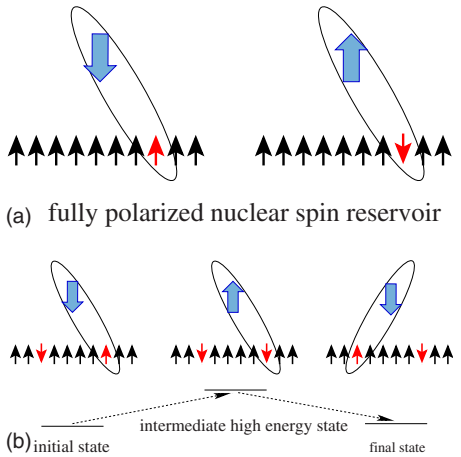

FIG. 3. (Color online) Schematic of possible spin exchange processes in case of fully polarized nuclei (upper panel) and one-spin-flipped nuclei (lower panel). For the fully polarized nuclei, the only possible process is the direct electron-nuclei flip-flop, which requires a large energy transfer to compensate in a high magnetic field. Second-order processes are also accessible for the one-spin-flipped nuclei. In this case, the high-energy state is an intermediate state, while the electron-spin state is not changed in the initial and final states, and two nuclear spins exchange their states.

and its width could both have $O(1/N)$ corrections. If the broadening of the spectral function is an $O(1)$ quantity, this amounts to an $O(1/N)$ correction that does not affect the resulting decay qualitatively. However, if the broadening of the spectral function is itself $O(1/N)$, as in the case of one-spin-flipped reservoir, the validity of $1/N$ expansion would be limited to times much shorter than $N*(N/A)\sim N$. In such a case, whether the spin correlation function completely decays at the time scale of $O(N)$ or not is beyond the current approximation. In particular, for shorter times with $t\sim O(1)$, a δ function spectral function and a narrowly broadened one (with a width of the order of $1/N$) cannot be distinguished. However, at longer time scales they are obviously different; one causes a complete decay, the other does not. This is why we do not try to predict the long-time behavior of the one-spin-flipped case.

The focus of this section is to illustrate the significance of the electron-mediated nuclear-spin flip-flops, to show how equation-of-motion approach can be used to solve this problem, and to connect the appearance of a continuous contribution to the spectral function at high energy to the appearance of the nuclear-spin flip-flops. Large-N approximation helps us to achieve all these goals. However, if an exact solution to the problem is desired, caution is needed. Indeed, a likely scenario for the one-spin-flipped-reservoir case is that the δ function in the fully-polarized-reservoir case is broadened into a narrow peak with an order $1/N$ width. This can be seen from a discussion of the eigenstates of the electron in a one-spin-flipped nuclear reservoir. Consider that out of N nuclear spins, we have n of them with hyperfine interaction similar to the $\bar{k}$ spin that is initially flipped. Therefore $n \ll N$ in a quantum dot because to have significant state mixing, we would need $A_k - A_{k'} \lesssim (A_k A_{k'})(2\omega_0 + A)$. This allows us to focus on the dynamics of these nuclear spins and the electron spin only. Due to angular momentum conservation, the only basis states we need to consider here are $|k\rangle = |\Downarrow, \uparrow, \ldots, \downarrow_k, \ldots, \uparrow\rangle$ and $|jj'\rangle = |\Uparrow, \uparrow, \ldots, \downarrow_j, \ldots, \downarrow_{j'}, \ldots, \uparrow\rangle$. $|k\rangle$ and $|jj'\rangle$ states are coupled by the hyperfine interaction, but within each group the Hamiltonian is diagonal. Furthermore, the two groups are separated by the electron Zeeman energy, which is the large energy scale in the current problem. As such, we can simplify the problem by building an effective Hamiltonian for only the $|k\rangle$ states because the initial state is one of them. This calculation can be done using the quasidegenerate perturbation theory.[49] The elements of the effective Hamiltonian are

$$H'_{kk} = E^0_{kk} - \frac{1}{2\omega_0 + A}\left(\sum_j^n A_j^2 + A_k^2\right),$$

$$H'_{kk'} = -\frac{A_k A_{k'}}{2\omega_0 + A}.$$

From the off-diagonal matrix elements, it is clear the dynamics of the system is completely due to the electron-mediated nuclear-spin flip-flop (the $|jj'\rangle$ states are the intermediate states). The state of the system at time t is

$$|\psi(t)\rangle = e^{-iHt/\hbar}|\psi(0)\rangle = \sum_k^n \langle k|e^{-iHt/\hbar}|\bar{k}\rangle|k\rangle.$$

For short times we can expand the time evolution operator to linear order and find

$$|\psi(t)\rangle \approx \sum_k^n \langle k|(1-iHt/\hbar)|\bar{k}\rangle|k\rangle = \left[1 - i\frac{\left(\sum_k^n A_k^2 + A_{\bar{k}}^2\right)t}{2\omega_0 + A}\right]|\bar{k}\rangle - i\sum_{k\neq\bar{k}}^n \frac{A_k A_{\bar{k}} t}{2\omega_0 + A}|k\rangle.$$

It is clear that for time $t \sim O(1)$, all the coefficients other than that for $|\bar{k}\rangle$ are of the order $1/N$, and the coefficient for $|\bar{k}\rangle$ is $\sim 1 - O(n/N)$; while at time $t \sim O(N)$, all the coefficients should be of order 1 and the decay of the initial state could be complete (notice that at that long time the linear expansion of the time evolution operator would not be valid anymore and a more accurate calculation or simulation would be needed). In short, for time $t \lesssim O(1)$, the electron-nuclear-spin state changes from the initial state only by an amount of the order $O(1/N)$, verifying our large-N expansion result presented in this section. For longer time of evolution, more accurate calculation or simulation is needed to obtain a clear physical picture.

In short, the example we have just considered, where an electron interacts with a polarized nuclear reservoir with one flipped spin, unequivocally connects the electron-mediated nuclear-spin flip-flop with the appearance of a continuous contribution at high frequency to the spectral function and the resulting decay of the electron-spin correlation function $G_\perp(t)$. It clearly illustrates the importance of the electron-mediated nuclear-spin flip-flop in the process of electron-spin decoherence. In Sec. III C we explore the effect of this process in the more general situations of partially polarized and unpolarized nuclear reservoirs.

C. Partially polarized and unpolarized nuclear reservoir

The solutions of both the fully polarized nuclear reservoir and one-spin-flipped nuclear reservoir are instructive, though they have little experimental relevance since the currently explored schemes of nuclear-spin polarization can only achieve up to 50% polarization.[13,50–53] It is thus important to find the solution for a general nuclear-spin configuration when studying the electron-spin decoherence.

Before we proceed further, we first define the effective nuclear polarization P

$$P = \frac{N_\uparrow - N_\downarrow}{N}. \tag{33}$$

Here $N_\uparrow$ ($N_\downarrow$) represents the number of nuclei in the spin-up (down) state (we have chosen z axis as our quantization axis). We further assume that both $N_\uparrow$ and $N_\downarrow$ are large, i.e., $N_\uparrow \sim N_\downarrow \sim O(N)$, which allows us to convert summations over both the up and down nuclear spins into integrals.

We treat the nuclear field (namely the Overhauser field) experienced by the electron spin, $\Sigma_k A_k I_k^z$, using the adiabatic approximation. When we choose to use this approximation, the sum will be treated as a c number instead of an operator, and factored out, no matter where it was in a correlation function (for example, $\Sigma A_{k'}\langle\langle I_k^- I_{k'}^z, S^z; S^+\rangle\rangle \approx \langle \Sigma A_{k'} I_{k'}^z\rangle_0 \langle\langle I_k^- S^z; S^+\rangle\rangle$). In a large effective magnetic field Ω, the electron spin precesses with frequency $\frac{\mu_B \Omega}{\hbar}$. In contrast, the nuclear field fluctuates around its average value by a small amount in a much slower time scale, since there are many nuclear spins ($N \gg 1$) interacting with the electron spin simultaneously and weakly, and the nuclear field evolves slowly compared to the time scale of the electron-spin dynamics. Our approximation is similar to the quasistatic approximation that has been used to describe the nuclear-spin reservoir.[17] Under this approximation we neglect the small time-dependent change in the nuclear field $\Sigma_k A_k I_k^z$, and factor it out from the time-dependent correlation function $\langle\langle \Sigma_k A_k I_k^z(t) S^-(t); S^+\rangle\rangle$. Meanwhile, the nuclear-spin raising and lowering operators are treated fully quantum mechanically. The term $\Sigma_k A_k I_k^z S^z$ in the Hamiltonian also remains as an operator for calculating commutators. When we treat a nuclear operator in the correlation functions as a c number, we always make sure that the difference from the real quantity only gives rise to higher-order contributions.

Similar to the highly polarized situations discussed previously, we study the solution in the low-energy and high-energy limits separately. Recall that in the case of polarized nuclear reservoir with one flipped spin, the weight of the delta function in the spectral function is reduced by a small amount of $O(1/N)$, and there appears a new continuous contribution to the spectral function near Ω because of the nuclear-spin flip-flop mediated by the electron. Since there is only one nuclear spin in the down state initially, the number of scattering channels for nuclear flip-flops is limited (see Fig. 3), so that decoherence effect of the continuous contribution is small, of the order $O(\frac{1}{N})$. With more nuclei in the down spin state, we expect that the continuous contribution become increasingly important, and potentially be of the order unity when $N_\downarrow \sim N_\uparrow$.

1. Low-energy solution

We again start with the low-energy end of the spectrum. The adiabatic approximation for the nuclear field allows us to write the first equation in Eq. (10) as

$$G_\perp(\omega) = -\frac{1}{\Omega} + \frac{1}{\Omega}\sum_k A_k \langle\langle I_k^- S^z; S^+\rangle\rangle_\omega + O\left(\frac{1}{\Omega^2}\right). \tag{34}$$

Thus the leading-order contribution to $G_\perp(\omega)$ is $O(\frac{1}{\Omega})$. Furthermore, the correlation function $\langle\langle I_k^- S^z; S^+\rangle\rangle_\omega$ represents processes in which real electron-nuclear-spin flip occurs. In other words, the low-energy behavior of $G_\perp(\omega)$ is determined by electron-spin-flip processes. The equations for $\langle\langle I_k^- S^z; S^+\rangle\rangle_\omega$ and $\langle\langle I_k^-; S^+\rangle\rangle_\omega$ are

$$\omega\langle\langle I_k^- S^z; S^+\rangle\rangle_\omega = -\frac{h_k}{2}G_\perp(\omega) + \frac{A_k}{4}\langle\langle I_k^-; S^+\rangle\rangle_\omega + \frac{1}{2}\langle\langle I_k^- V; S^+\rangle\rangle_\omega, \tag{35}$$

$$\omega\langle\langle I_k^-;S^+\rangle\rangle_\omega = A_k\langle\langle I_k^- S^z;S^+\rangle\rangle_\omega - h_k G_\perp(\omega), \tag{36}$$

with $h_k = A_k\langle I_k^z\rangle_0$ and $V = S^+\Sigma_k A_k I_k^- - \Sigma_k A_k I_k^+ S^-$. By introducing h_k, we are taking a mean-field average for the Overhauser field produced by this particular nucleus. This is equivalent to assuming a mixed nuclear-spin state of a particular polarization (instead of the pure nuclear-spin state we have used so far) and a slowly varying local nuclear-spin polarization consistent with the adiabatic approximation. Substituting Eq. (36) into Eq. (35), we obtain

$$\left(\omega^2 - \frac{A_k^2}{4}\right)\langle\langle I_k^- S^z;S^+\rangle\rangle_\omega = -\frac{h_k}{2}\left(\omega + \frac{A_k}{2}\right)G_\perp(\omega) + \frac{\omega}{2}\langle\langle I_k^- V;S^+\rangle\rangle_\omega. \tag{37}$$

Further calculation of $\langle\langle I_k^- V;S^+\rangle\rangle_\omega$ does not lead to any other higher-order correlation functions in the low-energy limit ($\omega \sim 1$). This is illustrated by the evaluation of both $\langle\langle I_k^- S^+ \tilde{I}^-;S^+\rangle\rangle_\omega$ and $\langle\langle I_k^- \tilde{I}^+ S^-;S^+\rangle\rangle_\omega$ with the EOM by a $1/N$ expansion. Here we have defined collective nuclear-spin operators $\tilde{I}_n^\pm = \Sigma_k A_k^n I_k^\pm$. The index n for $\tilde{I}$ is dropped when $n=1$. Neglecting all higher-order terms, we find

$$\Omega\langle\langle I_k^- S^+ \tilde{I}^-;S^+\rangle\rangle_\omega = -h_k\left\langle\left\langle \tilde{I}^-\left(\frac{1}{2} - S^z\right);S^+\right\rangle\right\rangle_\omega - \langle\tilde{I}_2^z\rangle_0\left\langle\left\langle I_k^-\left(\frac{1}{2} + S^z\right);S^+\right\rangle\right\rangle_\omega + \langle\langle I_k^- \tilde{I}^+ \tilde{I}^- S^z;S^+\rangle\rangle_\omega,$$

$$\Omega\langle\langle I_k^- \tilde{I}^+ S^-;S^+\rangle\rangle_\omega = -\left\langle I_k^- \tilde{I}^+\left(\frac{1}{2} - S^z\right)\right\rangle_0 - \langle\tilde{I}_2^z\rangle_0\left\langle\left\langle I_k^-\left(\frac{1}{2} + S^z\right);S^+\right\rangle\right\rangle_\omega + \langle\langle I_k^- \tilde{I}^+ \tilde{I}^- S^z;S^+\rangle\rangle_\omega, \tag{38}$$

where we have used the operator equality $S^+S^- = \frac{1}{2} + S^z$ and $S^-S^+ = \frac{1}{2} - S^z$, and the fact that $\langle\langle I_k^- S^+ \tilde{I}^-;S^+\rangle\rangle_\omega \sim O[\langle\langle I_k^- S^+ \tilde{I}_2^-;S^+\rangle\rangle_\omega]$. Combining Eq. (36) with Eq. (38), we find a single equation for $\langle\langle I_k^- S^z;S^+\rangle\rangle_\omega$ and $G_\perp(\omega)$,

$$\left(\omega^2 - \frac{A_k^2}{4}\right)\langle\langle I_k^- S^z;S^+\rangle\rangle_\omega = \frac{\omega A_k}{4\Omega}(1-P) + \left[-\frac{PA_k}{4}\left(\omega + \frac{A_k}{2}\right) + \frac{P^2 N A_k}{32\Omega}\right]G_\perp(\omega) + \frac{\omega P A_k}{4\Omega}\langle\langle \tilde{I}^- S^z;S^+\rangle\rangle_\omega - \frac{PA_k}{8\Omega}\langle\langle \tilde{I}_2^- S^z;S^+\rangle\rangle_\omega. \tag{39}$$

In this equation, we have used the mean-field average and replaced the nuclear-spin expectation value of the z component $\langle I_k^z\rangle_0$ by the average nuclear polarization $\frac{P}{2}$, basically assuming that nuclear-spin polarization is uniform inside the quantum dot. The summations $\Sigma_k A_k\langle\langle I_k^- S^z;S^+\rangle\rangle_\omega$ and $\Sigma_k A_k^2\langle\langle I_k^- S^z;S^+\rangle\rangle_\omega$ in Eq. (39) can be found by multiplying both sides of the equation by $\frac{A_k}{\omega^2 - A_k^2/4}$ or $\frac{A_k^2}{\omega^2 - A_k^2/4}$ and summing over k, which lead to

$$\langle\langle \tilde{I}^- S^z;S^+\rangle\rangle_\omega = \frac{16\omega(1-P)\sigma_2 + P[\sigma_2(2PN - 16\Omega\omega) - \sigma_3(8\Omega + P\sigma_3) + \sigma_4\sigma_2 P]G_\perp}{8(8\Omega - 2\omega P\sigma_2 + P\sigma_3)},$$

$$\langle\langle \tilde{I}_2^- S^z;S^+\rangle\rangle_\omega = \frac{8\omega(1-P)\sigma_3 + P[\sigma_3(PN - \omega P\sigma_3 - 8\Omega\omega) - \sigma_4(4\Omega - \omega P\sigma_2)]G_\perp}{4(8\Omega - 2\omega P\sigma_2 + P\sigma_3)}, \tag{40}$$

where

$$\sigma_n(\omega) = \sum_k \frac{A_k^n}{\omega^2 - \frac{A_k^2}{4}}. \tag{41}$$

Here $\sigma_n \sim N$ since it is a summation of $O(1)$ quantities over N nuclear spins (for a more detailed evaluation of σ_n, please see Appendix C). Plugging the result of Eq. (40) back into Eq. (39), we obtain an expression for $\Sigma_k A_k\langle\langle I_k^- S^z;S^+\rangle\rangle_\omega$, which can then be used to find $G_\perp(\omega)$ with Eq. (34). In the end, the low-energy solution for $G_\perp(\omega)$ is

$$G_\perp(\omega) = -8\frac{8\Omega - 2\omega\sigma_2 + P\sigma_3}{(8\Omega + P\sigma_3)^2 - P^2\sigma_2(2N + \sigma_4)}. \tag{42}$$

One important feature of the low-energy solution here is that, in terms of an approximate magnitude, $G_\perp(\omega) \sim O(\frac{1}{N})$, which is the same as in the cases of highly polarized nuclear reservoirs. Both spin-flip terms and an electron-mediated nuclear-spin flip-flop term (characterized by $\langle\langle I_k^- \tilde{I}^+ S^-;S^+\rangle\rangle_\omega$) contributed in the same order of magnitude to $G_\perp(\omega)$. The summation $\sigma_n(\omega)$ can be calculated with the same technique as we have used for calculating $\Sigma_0(\omega)$ with analytical continuation ($\omega \to \omega + i0^+$) and the conversion of summation to integral [$\Sigma_k \to \int_0^\infty d(\rho^2/R^2)$]. The real and imaginary parts of

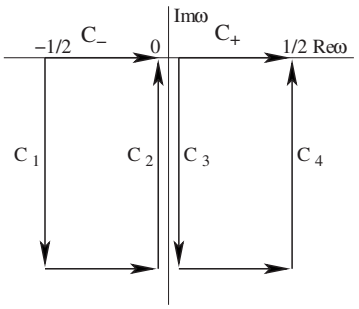

FIG. 4. To obtain the asymptotic behavior of $G_\perp(t)$ for partially polarized nuclei at long-time limit, the Fourier integral in Eq. (14) is converted into a Laplace integral by deforming the original contour C_+ and C_- into C_1, C_2, C_3, and C_4 as shown above and then allowing $\omega \to \infty$.

σ_n are evaluated and given in Appendix C. The real parts of σ_n have two branch cuts, one from 0 to $\frac{1}{2}$, and the other one from $-\frac{1}{2}$ to 0. The imaginary part of $G_\perp(\omega)$ is nonzero only in these regions.

With knowledge of $G_\perp(\omega)$, we can calculate its contribution to the temporal evolution of the spin correlation function $G_\perp(t)$ and to the long-time behavior. We first consider the case of zero external magnetic field, when $\Omega = \frac{PN}{2}$. Here large Ω implies that we are considering a finite nuclear polarization. To study the long-time behavior we again deform the original integration contours C_+ and C_- into C_1, C_2, C_3, and C_4 as in Fig. 4. The integrals at minus infinity in the lower half plane are neglected. Using the results of $\sigma_n(\omega)$ given in Appendix C, we find that the spectral function behaves as

$$\rho(0^{\mp} - is) = \frac{i(P \pm 1)}{2NP} \frac{1}{s \ln s} \tag{43}$$

on contour C_2 $(\omega = 0^- - is)$ and C_3 $(\omega = 0^+ - is)$ as s approaches 0^+. Thus the long-time asymptotic form of the Green's function contributed by the low-energy part of the spectrum is

$$G_\perp(t) \propto \frac{1}{PN} \frac{1}{\ln t}, \quad t \to \infty. \tag{44}$$

The long-time asymptotic form of $1/\ln t$ is the same as that of the fully polarized case (where there is no high-energy contribution in the spectral function to the inverse Fourier transform), and we do approach the correct numerical limit as $P \to 1$.

At the strong Zeeman field limit where $|\omega_0| \gg N$, there is no need for a finite nuclear polarization in order to satisfy the large-field condition. The Green's function $G_\perp(\omega)$ is proportional to $\frac{1}{\Omega}$ when $\omega \ll N$. The asymptotic behavior of $G_\perp(t)$ is $\frac{1}{t}$, and the decay amplitude is proportional to $\frac{1}{\Omega}$. Again this result agrees with the case of fully polarized nuclear reservoir.[19,22]

The properties of the low-energy spectrum of the spin correlation function studied in this subsection are quite similar to what have been investigated in previous studies.[19,22] The basic result is that the decay amplitude is of the order $O(\frac{1}{N})$ in the perturbative limit when the effective magnetic field is large (comparable to the effective number of nuclear spins in the QD). Since direct electron-nuclear-spin flip-flop is the main contributor to the low-energy end of the spectrum, it is quite reasonable that the magnitude of the spin correlation function in this regime is small, since the Zeeman energy mismatch is large at the large-field limit so that real electron-spin flip is unlikely.

2. High-energy solution

The high-energy region $(\omega \sim \Omega)$ for the spin correlation function $G_\perp(\omega)$ is of direct experimental relevance, because the electron-spin precession frequency is determined by the total effective field and is in the high-frequency region. In the case of a fully polarized nuclear reservoir, the contribution to the spectral function in the large-ω limit is a delta function that leads to completely coherent precession of the electron spin. When the effect of the electron-mediated nuclear-spin exchange is included in a one-spin-flipped reservoir, however, spin decoherence with a small amplitude arises. The key question now is whether this effect becomes large enough when initially the two nuclear-spin species (up and down) have roughly the same populations, so that it makes a measurable contribution to electron-spin dephasing. This question will be the focus of the following discussion of the high-energy solution for partially polarized and unpolarized nuclei.

We again use the adiabatic approximation for the nuclear field, and focus on the near-resonance region where $\omega = \Omega + O(1)$. In this region $\omega \gg A_k$, thus Eq. (12) can be simplified to

$$\left(\omega - \Omega - \frac{A_2}{4\Omega}\right) G_\perp(\omega) = 1 + \frac{1}{2\Omega} \sum_{k \neq k'} A_k A_{k'} \langle\langle I_k^- I_{k'}^+ S^-; S^+ \rangle\rangle_\omega, \tag{45}$$

where $A_2 = \Sigma_k A_k^2$. Correlation functions $\langle\langle I_k^- S^+ I_{k'}^-; S^+ \rangle\rangle_\omega$ have been neglected since they are much smaller in magnitude than $\langle\langle I_k^- I_{k'}^+ S^-; S^+ \rangle\rangle_\omega$: $\langle\langle I_k^- I_{k'}^+ S^-; S^+ \rangle\rangle_\omega$ is proportional to $\frac{1}{\omega - \Omega + (A_k - A_{k'})/2}$, while $\langle\langle I_k^- S^+ I_{k'}^-; S^+ \rangle\rangle_\omega$ is proportional to $\frac{1}{\omega + \Omega}$. In appearance, neglecting the smaller terms here is quite similar to the rotating wave approximation, where counter-rotating part is neglected.[43] Mathematically, the difference originates from the commutators of $S^\pm$ with S^z, i.e., $[S^\pm, S^z] = \mp S^\pm$. Since $\omega = \Omega + O(1)$, it is clear that $\frac{1}{\omega - \Omega + (A_k - A_{k'})/2} \sim O(1)$ while $\frac{1}{\omega + \Omega} \sim O(\frac{1}{2\Omega})$. Physically this difference is also easy to understand. In $\langle\langle I_k^- S^+ I_{k'}^-; S^+ \rangle\rangle_\omega$ an electron spin needs to be flipped down during its evolution. Such a real spin flip requires an energy transfer in the amount of electron-spin Zeeman energy, a large quantity in the current situation. On the other hand, in $\langle\langle I_k^- I_{k'}^+ S^-; S^+ \rangle\rangle_\omega$ there is no real electron-spin flip during the evolution, while at the end of the evolution two nuclear spins at k and k' have flip-flopped with each other. Therefore the correlation function $\langle\langle I_k^- I_{k'}^+ S^-; S^+ \rangle\rangle_\omega$ describes a nuclear-spin flip-flop process mediated by the electron. The energy required in this process is the difference of hyperfine coupling between the two nuclear sites k and k', much smaller than the electron Zeeman splitting. Equation (45)

clearly indicates that this is the only higher-order correlation function that contributes to $G_\perp(\omega)$ significantly within the approximation of large-N expansion.

The calculation of the one-pair correlation function $\langle\langle I_k^- I_{k'}^+ S^-; S^+\rangle\rangle_\omega$ involves the evaluation of two-pair correlation function $\langle\langle I_{k_1}^- I_{k_2}^+ I_{k_3}^- I_{k_4}^+ S^-; S^+\rangle\rangle_\omega$, which in turn depends on even higher-order correlation functions. This infinite recursive relationship is not a problem for the low-energy solution, where the terms of the one-pair correlation functions cancel each other out so that the transverse electron-spin Green's function only depends on the electron-nuclei spin-flip correlation functions $\langle\langle I_k^-; S^+\rangle\rangle_\omega$ and $\langle\langle I_k^- S^z; S^+\rangle\rangle_\omega$. In the present study of the high-energy regime, we focus on the high-field limit, when the effective field Ω is sufficiently large compared to N (meaning that the applied field is larger than the Overhauser field from a fully polarized nuclear-spin reservoir). At this limit the electron-spin self-energy can be expanded in powers of $\frac{N}{4\Omega}$. The infinite recursive relationship for nuclear-spin pair correlation functions can then be cut off, and the approximate solution for the electron-spin correlation function can be obtained with the first few terms in the expansion for the self-energy.[54]

We start with the exact EOM for the one-pair correlation function $\langle\langle I_k^- I_{k'}^+ S^-; S^+\rangle\rangle_\omega$,

$$\left(\omega - \Omega + \frac{A_k - A_k'}{2}\right)\langle\langle I_k^- I_{k'}^+ S^-; S^+\rangle\rangle_\omega = \frac{h_{k'}}{2}\langle\langle I_k^-; S^+\rangle\rangle_\omega - \frac{A_{k'}}{2}\langle\langle I_k^- S^z; S^+\rangle\rangle_\omega - \langle\langle I_k^- I_{k'}^+ \sum_{k''(k,k')} A_{k''} I_{k''}^- S^z; S^+\rangle\rangle_\omega. \tag{46}$$

The leading-order (in terms of $\frac{1}{\Omega}$) EOM for $\langle\langle I_k^- I_{k'}^+ \Sigma_{k''(k,k')} A_{k''} I_{k''}^- S^z; S^+\rangle\rangle_\omega$ takes the form

$$\omega\langle\langle I_k^- I_{k'}^+ \sum_{k''(k,k')} A_{k''} I_{k''}^- S^z; S^+\rangle\rangle_\omega = -\frac{A_2}{4}\langle\langle I_k^- I_{k'}^+ S^-; S^+\rangle\rangle_\omega - \frac{A_k}{4}\langle\langle I_{k'}^+ \sum_{k''(k,k')} A_{k''} I_{k''}^- S^-; S^+\rangle\rangle_\omega, \tag{47}$$

where two-pair correlation functions have been neglected. In leading order of $1/\Omega$, the EOMs of the two lowest-order correlation functions of electron-nuclei flip-flopping in Eq. (10) are simplified to

$$\langle\langle I_k^-; S^+\rangle\rangle_\omega = -\frac{P}{2\Omega} A_k G_\perp(\omega), \tag{48}$$

and

$$\langle\langle I_k^- S^z; S^+\rangle\rangle_\omega = -\frac{A_k}{4\Omega} G_\perp - \frac{1}{2\Omega}\langle\langle I_k^- \sum_{k'(k)} A_{k'} I_{k'}^+ S^-; S^+\rangle\rangle_\omega. \tag{49}$$

Combining Eq. (46) with Eqs. (48) and (49) we find the following equation for the one-pair nuclear-spin flip-flop correlation function $\langle\langle I_k^- I_{k'}^+ S^-; S^+\rangle\rangle_\omega$,

$$\left(\tilde{\omega} + \frac{A_k - A_{k'}}{2}\right)\langle\langle I_k^- I_{k'}^+ S^-; S^+\rangle\rangle_\omega = \frac{1-P^2}{8\Omega} A_k A_{k'} G_\perp(\omega) + \frac{A_{k'}}{4\Omega}\langle\langle I_k^- \sum_{k''(k,k')} A_{k''} I_{k''}^+ S^-; S^+\rangle\rangle_\omega + \frac{A_k}{4\Omega}\langle\langle I_{k'}^+ \sum_{k''(k,k')} A_{k''} I_{k''}^- S^-; S^+\rangle\rangle_\omega, \tag{50}$$

with $\tilde{\omega} = \omega - \Omega - \frac{A_2}{4\Omega}$ representing the deviation of the frequency from Ω in the high-energy limit, and $A_2/\Omega \sim O(1)$. Equation (50) cannot be solved exactly because of the summation on the right-hand side. Here we seek an approximate solution in the leading order of $\frac{N}{\Omega}$ in the high-field (large Ω) limit as we mentioned before ($\Omega \gg N$). At this limit the last two terms on the right-hand side of Eq. (50) make a higher-order contribution and can be neglected. Dividing both sides of Eq. (50) by $\tilde{\omega} - \frac{A_k - A_{k'}}{2}$ and summing over k', we obtain (recall that $\tilde{I}^+ = \Sigma_k A_k I_k^+$)

$$\langle\langle I_k^- \tilde{I}^+ S^-; S^+\rangle\rangle_\omega = \left[\frac{1-P^2}{8\Omega} A_k \sum_{k'} \frac{A_{k'}^2}{\tilde{\omega} + \frac{A_k - A_{k'}}{2}} + O\left(\frac{N^2}{16\Omega^2}\right)\right] G_\perp(\omega). \tag{51}$$

$\langle\langle \tilde{I}^- I_{k'}^+ S^-; S^+\rangle\rangle_\omega$ can be calculated with a similar approach,

$$\langle\langle \tilde{I}^- I_{k'}^+ S^-; S^+\rangle\rangle_\omega = \left[\frac{1-P^2}{8\Omega} A_{k'} \sum_{k} \frac{A_k^2}{\tilde{\omega} + \frac{A_k - A_{k'}}{2}} + O\left(\frac{N^2}{16\Omega^2}\right)\right] G_\perp(\omega). \tag{52}$$

We then substitute Eqs. (51) and (52) into Eq. (50) to obtain the solution for the one-pair correlation function $\langle\langle I_k^- I_{k'}^+ S^-; S^+\rangle\rangle_\omega$. Finally we use Eq. (45) to find the Green's function in the high-energy limit. The result is

$$G_\perp(\omega) = \frac{1}{\tilde{\omega} - \frac{1-P^2}{16\Omega^2}\Sigma_1(\tilde{\omega}) - \frac{1-P^2}{64\Omega^3}[\Sigma_2(\tilde{\omega}) + \Sigma_3(\tilde{\omega})]}, \tag{53}$$

where

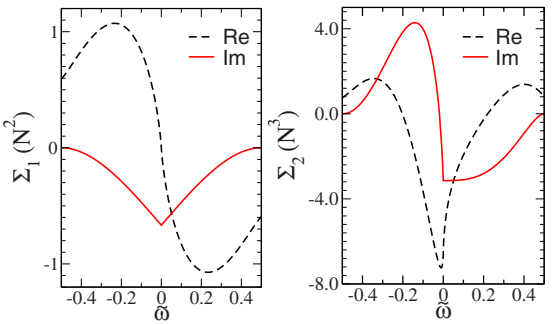

FIG. 5. (Color online) The self-energies $\Sigma_1(\tilde{\omega})$ (left panel) and $\Sigma_2(\tilde{\omega})$ (right panel) as functions of $\tilde{\omega}=\omega-\Omega-A_2/\Omega$. In these numerical calculations, we have assumed that the hyperfine coupling constant takes the form as in Eq. (2). Both the real part (dashed line) and imaginary part (solid line) of the self-energies are plotted.

$$\Sigma_1(\tilde{\omega}) = \sum_{k,k'} \frac{A_k^2 A_{k'}^2}{\tilde{\omega} + \dfrac{A_k - A_{k'}}{2}}, \tag{54}$$

$$\Sigma_2(\tilde{\omega}) = \sum_{k,k',k''} \frac{A_k^2 A_{k'}^2 A_{k''}^2}{\left(\tilde{\omega} + \dfrac{A_k - A_{k'}}{2}\right)\left(\tilde{\omega} + \dfrac{A_k - A_{k''}}{2}\right)}, \tag{55}$$

$$\Sigma_3(\tilde{\omega}) = \sum_{k,k',k''} \frac{A_k^2 A_{k'}^2 A_{k''}^2}{\left(\tilde{\omega} + \dfrac{A_k - A_{k'}}{2}\right)\left(\tilde{\omega} + \dfrac{A_{k''} - A_{k'}}{2}\right)}. \tag{56}$$

$\Sigma_1(\tilde{\omega})$ has two summations over nuclear spins, thus $\Sigma_1(\tilde{\omega}) \sim N^2$. For the same reason, $\Sigma_2(\tilde{\omega})$ and $\Sigma_3(\tilde{\omega})$ are proportional to N^3. In the above derivation, we have neglected the difference between $\Sigma_{k''(k,k')}$ and $\Sigma_{k''}$, which only gives an order unity contribution to the three self-energy terms. The final expression of $G_\perp(\omega)$ we have found in Eq. (53) is of order $O(1)$, in contrast to the solution in the low-energy limit, which is of order $O(1/N)$.

In Appendix D, we give the details on how to evaluate the self-energy terms $\Sigma_1(\tilde{\omega})$, $\Sigma_2(\tilde{\omega})$, and $\Sigma_3(\tilde{\omega})$. Figure 5 shows our results for the self-energy. Specifically, we plot the real and imaginary parts for both of the self-energy terms as functions of the shifted frequency $\tilde{\omega}$. We can see that there is a cusp at $\tilde{\omega}=0$ for the imaginary parts of both $\Sigma_1(\tilde{\omega})$ and $\Sigma_2(\tilde{\omega})$. A closer look at $\Sigma_1(\tilde{\omega})$ shows that Im $\Sigma_1(\tilde{\omega})$ is negative for the whole region of $\tilde{\omega}$, which ensures that the spectral function $\rho(\tilde{\omega})$ is always positive. Like Im $\sigma_n(\omega)$ [see Eq. (41) and Appendix C], which is nonzero when $-\frac{1}{2}<\omega<\frac{1}{2}$, Im $\Sigma_1(\tilde{\omega})$ does not vanish when $-\frac{1}{2}<\tilde{\omega}<\frac{1}{2}$. The behavior of $\Sigma_2(\tilde{\omega})$ is different from $\Sigma_1(\tilde{\omega})$. Neither the real nor the imaginary part of $\Sigma_2(\tilde{\omega})$ is symmetrical about $\tilde{\omega}=0$. On the other hand, Im $\Sigma_2(\tilde{\omega})$ changes sign near $\tilde{\omega}=0$. This leads to no contradiction because $\Sigma_2(\tilde{\omega})$ is a higher-order correction term to $\Sigma_1(\tilde{\omega})$, so that $\Sigma_2(\tilde{\omega})$ by itself has no physical meaning. Figure 5 shows that the absolute values of $\Sigma_2(\tilde{\omega})$ are generally larger than those of $\Sigma_1(\tilde{\omega})$. However, these two

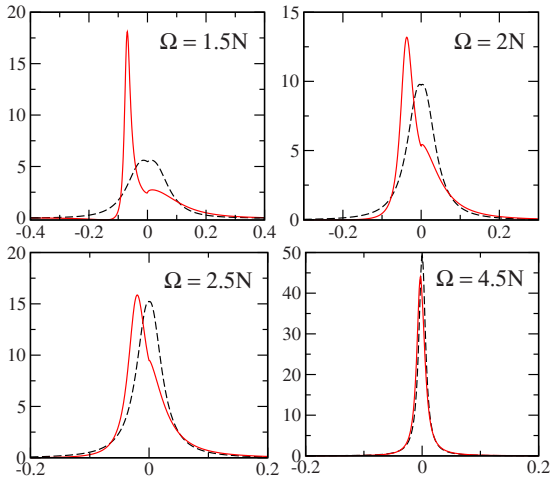

FIG. 6. (Color online) The spectral function $\rho(\tilde{\omega})$ in the high-energy limit as a function of the shifted frequency $\tilde{\omega}$. We have plotted the spectral function for $\Omega=1.5N$, $2N$, $2.5N$, and $4.5N$. In each of these cases, we have calculated $\rho(\tilde{\omega})$ with two approximations. In the first one, we have evaluated $\rho(\tilde{\omega})$ with only $\Sigma_1(\tilde{\omega})$ (dashed line), and in the other one, we have used both $\Sigma_1(\tilde{\omega})$ and $\Sigma_2(\tilde{\omega})$ (solid line). The lower figures clearly show the success of our large-field expansion method. These plots also illustrated the idea that the original delta function in the spectral function is broadened to a continuous spectral function after the virtual nuclear-spin flip-flop is included in the calculations.

self-energy terms are multiplied by $\frac{N^3}{64\Omega^3}$ and $\frac{N^2}{16\Omega^2}$, respectively, in Eq. (53), so that $\Sigma_1(\tilde{\omega})$ is still the largest contribution to the electron-spin self-energy.

So far the two-pair correlation function has been neglected when deriving the EOMs. If we keep the two-pair correlation function and all the other corresponding functions of the same order, but neglect the three-pair correlation functions, we find two more higher-order self-energy terms which are proportional to $\frac{N^4}{(4\Omega)^4}$ and $\frac{N^5}{(4\Omega)^5}$. In principle, we can perform the large-field expansion to higher and higher orders. Eventually we should arrive at a finite geometrical series of $\frac{N}{4\Omega}$. The series should be finite because there is a finite number (N) of nuclear spins in the quantum dot, and there can be at most $N_\downarrow$ ($N_\uparrow$) pairs of flip-flopping nuclear spins if $N_\downarrow < N_\uparrow$ ($N_\uparrow < N_\downarrow$). This gives rise to a natural cutoff of self-energy terms in our large-field expansion. However, even extension of the calculation to the order of $\frac{N^4}{(4\Omega)^4}$ and $\frac{N^5}{(4\Omega)^5}$ is already very complicated within the current approach. Nevertheless, the approximation with the first two self-energy terms should be accurate enough as long as the total effective magnetic field Ω is large compared with N (representing the Overhauser field produced by a polarized nuclei spin reservoir).

The validity of our large-field expansion method is illustrated in Fig. 6, where we have plotted the electron-spin spectral function $\rho(\tilde{\omega})$ for various effective fields Ω. For a direct comparison, we have calculated $\rho(\tilde{\omega})$ using only the self-energy term $\Sigma_1(\tilde{\omega})$, and using both $\Sigma_1(\tilde{\omega})$ and $\Sigma_2(\tilde{\omega})$. In the two upper panels of the figure, where Ω is not very large ($1.5N$ and $2N$), the contribution of $\Sigma_2(\tilde{\omega})$ is comparable to $\Sigma_1(\tilde{\omega})$. In these cases one needs to calculate more higher-

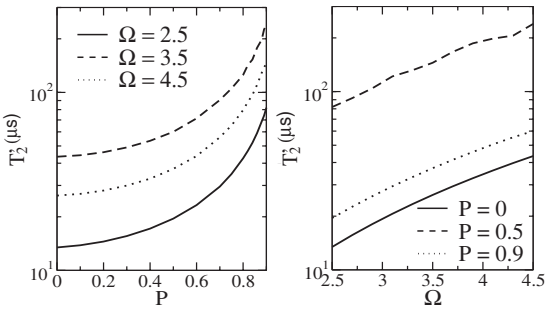

FIG. 7. The electron spin T_2' time in logarithmic scale as a function of nuclear-spin polarization P (left panel) and the effective magnetic field Ω (right panel). The three curves in the left panel correspond to three different total effect fields, which for a particular polarization would correspond to different external fields. The three curves in the right panel are for three different nuclear polarizations. The number of nuclear spins for all the curves is $N=10^5$. T_2' is estimated from the spectral function by finding the half-width of the spectral peak. It is equivalent to the free-induction decay time of the electron spin. The coherence time is greatly enhanced by increasing the nuclear polarization to 90%. We have assumed $A=92$ μeV in these calculations. Correspondingly, for $N=10^5$, the electron hyperfine coupling with individual nuclear spins is of the order $O(A/N)\sim 1$ neV, while the corresponding time scale is $O(N/A)\sim 1$ μs. For a different N the energy and time scales vary accordingly.

order terms in the expansion of self-energy to achieve convergence. When $\Omega=2.5N$, the difference is already not very significant. When $\Omega=4.5N$, we can clearly see that the contribution of $\Sigma_2(\tilde{\omega})$ is negligible. Therefore, our results should be quite accurate as long as $\Omega\geq 2.5N$. For unpolarized nuclei, $\Omega=2.5N$ corresponds roughly to an external field of 10 T for GaAs dots.[45] We have also checked the sum rule for the spectral function, which should satisfy $\int_{-\infty}^{\infty}\rho(\tilde{\omega})d\tilde{\omega}=1$, in all the numerical calculations. We find that the sum rule is always accurate to within 10^{-3}.

A significant feature of Fig. 6 is that the original delta function $\delta[\omega-\Omega+O(1)]$ without decoherence has been broadened into a continuous (though sharply peaked) spectrum after the electron-mediated flip-flops of nuclear spins are considered. The sum rule from the continuous spectrum clearly indicates that there is no contribution from a delta function to the spectral function, so that the decay of $G_\perp(t)$ should be complete.

Once the spectral function is obtained, the relaxation time T_2' (Ref. 55 gives a brief discussion of definitions of various decay times) for the electron-spin correlation function $G_\perp(t)$, which represents the dephasing time scale of a freely evolving electron spin in an effective magnetic field (free-induction decay, or FID), can be estimated as the inverse of the half-width of the spectrum at the $\tilde{\omega}=0$ peak, i.e., $T_2'=1/\Delta\tilde{\omega}$. The result is shown in Fig. 7, where the dephasing time is plotted as functions of the nuclear polarization P and the effective magnetic field Ω. In all the numerical calculations, we have assumed that the total hyperfine coupling strength is $A=\Sigma_k A_k=92$ μeV. Figure 7 indicates that both polarizing the nuclear spins and increasing the external magnetic field can enhance the spin coherence time T_2'. In essence, increasing P leads to a reduced phase space for nuclear-spin flip-flop, while increasing Ω leads to increased energy for the intermediate state and thus reduced cross section for the higher-order processes. The T_2' time can be enhanced by 1 order of magnitude by increasing P from 0 to 90%, while applying higher magnetic fields extends the coherence time by a few times. For unpolarized nuclei with $\Omega=2.5N$ and $N=10^5$ (10^5 nuclei in the quantum dot), we find $T_2'\approx 10$ μs, which is similar to the decoherence time caused by the nuclear dipole-dipole interaction at a comparable external field.[20] This comparison needs to be kept in perspective, however, since our numerical results are obtained for a quasi-two-dimensional QD with a Gaussian radial wave function, while the previous results for dipolar coupling are obtained for a three-dimensional QD.[20] In addition, our results are obtained by assuming nuclear spin $I=\frac{1}{2}$ throughout this paper, even though all the isotopes of Ga and As nuclei have spin $I=\frac{3}{2}$. While exploration of the dimension and I dependence of T_2' would be interesting, we do not anticipate qualitative differences arising from these detailed features.

The electron-spin free-induction decay due to electron-mediated nuclear-spin flip-flop has been studied in Ref. 28, which solved directly for the time evolution of the electron-spin density matrix. Our results presented in Fig. 7 are consistent with what was presented in Fig. 2 of Ref. 28, in the sense that the decay times obtained are of the same order, and have qualitatively the same dependence on the number of nuclear spins. The consistency between these two studies, which use very different methods, is evidence that both results are reliable representations of the real physical processes.

The calculated T_2' time is proportional to the time unit N/A. Therefore a larger quantum dot [with a larger number of nuclear spins (larger N)] has a longer T_2' time. In the bulk limit the coherence time of a conduction electron becomes infinitely large due to the mechanism we consider here, because the hyperfine coupling is homogeneous so that there is no fluctuation of nuclear field. In the limit of a smaller quantum dot the profile of the electron wave function becomes sharper due to the strong confinement. One thus also anticipates increased T_2' time since the effective nuclear flip-flop is more difficult to realize energetically, similar to the case of the dipolar coupling.[20] These limiting cases indicate that there should be a certain QD size where decoherence effect of the nuclear reservoir is the most serious. However, in our present calculations we cannot reach the small-dot limit. When we convert the sums over nuclear sites into integrals, we lose the information that variation of hyperfine coupling strength among the nuclear spins is actually discrete instead of continuous.

The real time dynamics of the transverse electron-spin Green's function $G_\perp(t)$ can be obtained by performing the inverse Fourier transform using Eq. (14). In Fig. 8 we show the evolution of the envelope of $G_\perp(t)$ (its maximum values during each cycle) for various nuclear polarization P and total field Ω combinations. The actual evolution of $G_\perp(t)$ oscillates coherently with a frequency close to Ω (for example, in GaAs, at 10 T effective field, the period of the electron-spin precession is about 17 ps). In the relative small-magnetic-field ($\leq$10 T) and low-polarization limit,

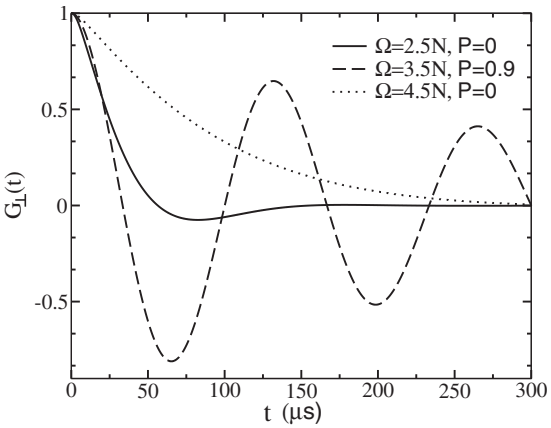

FIG. 8. The real part of the Green's function $G_\perp$ for different regime of T_2'. $G_\perp$ is evaluated by performing the inverse Fourier transform with Eq. (14). We have only plotted the envelope function of the correlation function. The actual evolution should be modulated by a fast oscillation with frequency Ω. As in previous figures, $N=10^5$.

the amplitude of $G_\perp(t)$ decays rapidly and completely. On the other hand, the coherence of the electron spin can be maintained for a much longer period if $P=0.9$ even without a very large Ω (i.e., a small external field). While 90% nuclear polarization may seem difficult to achieve using dynamical nuclear polarization by polarized electronic transport[51,53,56] or circularly polarized photons[50,57,58] through hyperfine interaction, the difficulties are in practice, not in principle. Our approximation should still be accurate with such a large nuclear polarization, because the numbers of up and down nuclear spins are still in the same order of magnitude at $P=0.9$. If we go to the extremely polarized limit, the decoherence effect should become suppressed, as in the case of fully polarized nuclei. For the curve with $P=0.9$, we also observe a clear revival for $G_\perp(t)$ even after 100 μs. This recoherence of the electron spin from the nuclear spins at high polarization is an illustration of the nuclear spins as a quantum coherent memory,[39] even though the electron and nuclear spins are far from on-resonance in the present study.

We can identify the long-time asymptotic behavior of $G_\perp(t)$ as before. Again, the contour shown in Fig. 4 can be used to calculate the asymptotic integrals of Eq. (14) as $t\to\infty$ with the method of steepest descent. For simplicity we only include the effect of $\Sigma_1(\tilde{\omega})$. To evaluate these integrals we need to find the asymptotic form of the spectral function. The calculation is similar to what we have done for the low-frequency solution. On the contours of C_2 and C_3 in Fig. 4, we define $\tilde{\omega}=0^{\mp}-is$. On the contours of C_1 and C_4, we replace $\tilde{\omega}$ by $\mp\frac{1}{2}-is$, where s is a new real variable. The long-time ($t\to\infty$) behavior is determined by the asymptotic form of the spectral function as $s\to 0^+$. On C_2 and C_3, we find

$$\rho(0^{\mp}-is)=\frac{24\Omega^2}{\pi^2(1-P^2)N^2}(1\mp 3is)+O(s^3). \tag{57}$$

Performing the integral along the contours C_2 and C_3 as $t\to\infty$, we find

$$G_\perp(t)\propto\frac{144\Omega^2}{\pi^2(1-P^2)N^2}\frac{1}{t^2}. \tag{58}$$

On the contours C_1 and C_4, $\rho(\mp\frac{1}{2}-is)\propto s^2$. Therefore, the integrals along C_1 and C_4 have a contribution of $\frac{1}{t^3}$, which is negligible compared to $\frac{1}{t^2}$ at the long-time limit. This nonexponential long-time decay behavior is faster than that of the low-energy solution with strong magnetic field, where a time dependence of $\frac{1}{t}$ is found. The $\frac{1}{t^2}$ behavior here is obtained by only considering $\Sigma_1(\tilde{\omega})$. The inclusion of $\Sigma_2(\tilde{\omega})$ is beyond the current study. However, we would expect power-law decay instead of the $\frac{1}{\ln t}$ decay that appears in the solution for the low-energy solution in the absence of external magnetic field. Qualitatively, the nuclear-spin flip-flop induced electron-spin dephasing leads to a faster decay ($\sim 1/t^2$) of the spin correlation function, then at long times a slower (and also smaller amplitude) decay due to direct electron-nuclear-spin flip-flop dominates.

Notice that the expression in Eq. (58) diverges as the nuclear polarization goes toward 1. However, this is insignificant since our discussions in this subsection apply to partially and unpolarized nuclei so that P is always less than 1. Instead, the low-energy solution has the right asymptotics when $P=1$. This is because both the exact solution of fully polarized nuclei and the low-energy solution include only the real electron-nuclei flip-flop, while the high-energy solution found in this section is due completely to the higher-order processes, which are only significant when $P<1$.

Near the end of Sec. III B 2 we commented that the large-N expansion leads to an expression (a δ-function component for the spectral function) that cannot be used at the long-time limit for the one-spin-flipped nuclear reservoir. The partially-polarized-reservoir case we consider in this section is quite different. Here large-N expansion leads to an order $O(1/N)$ correction to a finite $O(1)$ broadening in the spectral function, so that at the large time limit the correction is still $O(1/N)$ and therefore quantitative, while in the previous case the $O(1/N)$ "correction" is on a zero broadening, which can lead to qualitatively different behavior at the long-time limit. More specifically, the large-N expansion is used here in obtaining Eq. (45), which keeps only the correlation function $\langle\langle I_k^- I_{k'}^+ S^-;S^+\rangle\rangle_\omega$ that represents one-pair flip-flops for the nuclear spins. Then the approximation is used again as we simplify the calculation of $\langle\langle I_k^- I_{k'}^+ S^-;S^+\rangle\rangle_\omega$, where we cut off the contributions from the multiple-pair contributions. In both cases the large-N expansion is used essentially to constrain ourselves to the one-pair flip-flop situation, which we anticipate to be the dominant contribution to the nuclear-spin dynamics at larger fields.

Our results in Sec. III C do in general have a finite validity range in the time scale, because we used adiabatic approximation for the Overhauser field from the nuclear spins. Recent experimental study shows that for quantum dots of reasonable size ($\lesssim$100 nm), the relaxation time of dynamically generated Overhauser field is on the order of tens of seconds to minutes,[13,51,52] much longer than any electron-spin time scale we are interested in (consider that for 10^5 nuclei, the time unit is on the order of μs and $O(N)$ time

would be 0.1 s). In the absence of dynamical nuclear-spin polarization, the Overhauser field is of the order $O(\sqrt{N})$ ($\sim$mT), much smaller than the total effective field Ω that is of order $O(N)$ (>5 T in GaAs). In this case the validity range for our results is essentially infinite in terms of qualitative behaviors.

IV. DISCUSSION

Our calculations presented in this paper can be generalized in several ways. First, although we have been dealing with nuclei of spin $\frac{1}{2}$ exclusively throughout this paper, our study can be extended to nuclei with higher spin values. Although larger I means inevitably more complexity in the algebra, we do not expect the qualitative behavior of the spectral function and the long-time decay we have discovered here be modified in any significant manner. Second, we have assumed a relatively simple form of the hyperfine coupling constant as a function of the position of the nucleus at $\mathbf{r}_k=(\rho_k,\theta,z)$, i.e., $A_k=e^{-\rho_k^2/R^2}$, to simplify the algebra. This form of A_k corresponds to a quasi-two-dimensional quantum dot with a Gaussian radial wave function. However, our derivations and approximations are not limited by this choice of A_k and are applicable to any form of quantum dot with arbitrary electronic wave function. In short, all our results before converting the summations into integrals are correct for a general electron wave function. Generalization to a three-dimensional quantum dot is more complicated mathematically because one would encounter integrations that can only be performed numerically when converting the sums over nuclear lattice sites to integrals.

A more challenging and interesting generalization of the present work is to consider smaller effective magnetic fields, for example with $\Omega\sim O(\sqrt{N})$, which is the order of magnitude for the thermal statistical nuclear magnetic field.[59] In such a case, our large N expansion is still valid, because $\sqrt{N}$ is still much larger than A_k. The Zeeman energy mismatch dictates that the direct electron-nuclei relaxation effect is still negligible. However, the large-field expansion we have used in the case of unpolarized nuclear reservoir loses its power in this situation since the expansion parameter $\frac{N}{\Omega}\gg 1$. Basically one has to consider more higher-order correlation functions with more pairs of flip-flopping nuclear spins. An alternative approach needs to be developed for analytical solutions.

Our study assumes that the nuclear-spin reservoir is in an initial product state, although when we take mean-field averages for the Overhauser field, we are essentially using mixed (product) states for the nuclear spins. It has recently been found that electron-spin dynamics shows different behaviors for randomly correlated initial nuclear-spin states or ensemble averaged initial states.[18] We expect that our analytical results can be directly used to investigate the electron-spin decoherence by summing over these more complicated product states in an ensemble. Our treatment can also be applied to study the non-Markovian spin dynamics of spin-boson model, where a single spin interacts with a reservoir of bosons at thermal equilibrium in the initial state. It would also be interesting to extend the approach presented in this paper to study the dephasing time of two-electron spin states in double QD, where both the T_2^* and T_2 have been measured.[4]

The coherent properties calculated in this work are directly related to experimental measurements of electron-spin free-induction decay and do not include possible effects of spin echoes, which can help recover quantum coherence into the electron-spin system. It has been pointed out that the lowest-order effect of the electron-mediated nuclear-spin flip-flop can be corrected by spin echoes.[24,32] Within the correlation function approach, a particular choice of a spin echo would require the introduction of a corresponding spin correlation function. Consequently a new set of equations of motion has to be set up and solved.

V. CONCLUSIONS

In summary, we have developed an equation-of-motion approach to study the coupled dynamics of an electron spin interacting with a nuclear-spin reservoir through contact hyperfine interaction. In particular, we have identified the electron-spin Green's function $G_\perp(t)$ that contains full information of electron-spin coherence, and obtained a set of equations of motion for this and a group of other correlation functions for the electron and nuclear spins.

In the current study we particularly focused on the relaxation properties of $G_\perp(t)$ at the limit of a large effective magnetic field. We have solved this problem for three types of initial nuclear-spin states: the fully polarized case, the almost fully polarized case with one nuclear spin flipped, and the more general partially polarized and unpolarized cases. By comparing the exact solution of a fully polarized nuclear reservoir and the solution of an almost fully polarized case, we demonstrate that the electron-mediated nuclear-spin flip-flop is an important mechanism of electron-spin decoherence. Physically, the single confined electron mediates flip-flop of nuclear spins in the quantum dot. The resulting nuclear-spin dynamics back-acts on the electron spin via the Overhauser field in the form of a fluctuating effective magnetic field, which leads to pure dephasing in the electron spin. Our studies of electron-spin decoherence in the low-energy region recover previously obtained results by other groups. Most importantly, we have obtained the solution of partially polarized and unpolarized nuclei by considering the indirect nuclear-spin flip-flop explicitly, helped with a large-field expansion method. We find that relaxation of electron-spin coherence is very sensitive to nuclear polarization when $P>0.6$, and the electron-spin coherence time can be enhanced by ten times if the nuclear polarization is increased to 90%. We also find that this loss of coherence is complete, and the long-time asymptotic behavior of the Green's function representing the transverse electron-spin dynamics is $\frac{1}{t^2}$.

ACKNOWLEDGMENTS

We acknowledge financial support by NSA and LPS through USARO Grant No. DAAD190310128. We also thank useful discussions with Jacob Taylor, Renbao Liu, and Wayne Witzel.

APPENDIX A: EXACT SOLUTION OF THE ELECTRON-SPIN STATE IN A FULLY POLARIZED NUCLEAR-SPIN RESERVOIR IN THE JORDAN-WIGNER REPRESENTATION

The problem of an electron spin coupled with a fully polarized nuclear-spin reservoir via contact hyperfine interaction can be mapped exactly to the noninteracting Anderson impurity model. To demonstrate this connection, we first introduce the Jordan-Wigner representation, employing a set of fermionic operators to replace the spin operators:[60]

$$S^+ = d, \quad S^- = d^\dagger, \quad S^z = \frac{1}{2} - n_d,$$

$$I_k^+ = e^{-i\pi n_d} a_k, \quad I_k^- = a_k^+ e^{i\pi n_d}, \quad I_k^z = \frac{1}{2} - n_k, \tag{A1}$$

where $n_d = d^\dagger d$ and $n_k = a_k^\dagger a_k$. All operators obey the standard fermion anticommutation relations: $\{d, d^\dagger\} = 1$; $\{a_k, a_k^\dagger\} = 1$. This representation preserves all spin commutation relations except for those of two nuclear-spin operators at two different lattice sites. However, these commutators are not needed for a fully polarized nuclear reservoir, because there should be only one flipped spin at any moment during the evolution. In terms of correlation functions, this means that we will not encounter any correlation function containing two nuclear operators, so that there is no need of ordering different nuclear-spin operators using the fermion operators.

Transforming the original spin Hamiltonian of Eq. (1) into the new representation, we arrive at

$$H_{\mathrm{JW}} = -\sum_k \frac{A_k}{2} n_k - \left(\omega_0 + \frac{A}{2}\right) n_d + \sum_k \frac{A_k}{2} (a_k^\dagger d + d^\dagger a_k), \tag{A2}$$

where $A = \Sigma_k A_k$. We have ignored a constant term in the derivation. The quartic interaction term $\Sigma_k A_k n_k n_d$ in H_{JW} vanishes because $\Sigma_k A_k n_k$ and n_d cannot both be 1 (down state). The new Hamiltonian H_{JW} is in the form of the noninteracting Anderson impurity model,[47] describing a localized state (electron spins) interacting with a semicontinuous state spectrum (representing the nuclear spins). This is the key feature that we focus on in this paper: a single electronic spin interacts with many nuclear spins with different strengths. The noninteracting Anderson impurity model can be solved exactly. Specifically, the exact solution of H_{JW} for the Green's function $\langle\langle d; d^\dagger\rangle\rangle_\omega$ is[46]

$$\langle\langle d; d^\dagger\rangle\rangle_\omega = \frac{1}{\omega + \omega_0 + \frac{A}{2} - \frac{1}{4}\sum_k \frac{A_k^2}{\omega + \frac{A_k}{2}}}. \tag{A3}$$

The spectral function $(-\mathrm{Im}\langle\langle d; d^\dagger\rangle\rangle_\omega/\pi)$ represents the overlapping of the localized state with the exact eigenstate, and is the same as what we have found in Sec. III.

APPENDIX B: EOMS FOR AN ELECTRON IN A POLARIZED NUCLEAR RESERVOIR WITH ONE NUCLEAR SPIN FLIPPED

The EOMs of one electron spin interacting with a polarized nuclear reservoir with one flipped spin are generated by computing the commutators in Eq. (9). The highest-order correlation functions that survive are those that involve two spin-lowering operators, either S^- or I_k^-. All higher-order functions with more spins flipped to down direction vanish because the total angular $(\Sigma_k I_k^z + S^z)$ momentum along z direction (of the external field) is a constant of motion. Explicitly, the equations are

$$\left[\omega - \Omega_0 - \Sigma_0(\omega) + A_k + \frac{A_k^3}{4(\omega^2 - A_k^2/4)}\right]\langle\langle n_k S^-; S^+\rangle\rangle_\omega = \langle\Psi_0|n_k|\Psi_0\rangle - \frac{1}{4}\sum_{k'(k)} \frac{A_k A_{k'} V_{kk'}(\omega)}{\omega + A_k/2} - \frac{1}{4}\sum_{k'(k)} \frac{A_k A_{k'} V_{k'k}(\omega)}{\omega - A_{k'}/2}, \tag{B1}$$

$$\left(\omega - \frac{A_{k'}}{2}\right)\langle\langle n_k I_{k'}^-; S^+\rangle\rangle_\omega = -\frac{A_{k'}}{2}\langle\langle n_k S^-; S^+\rangle\rangle_\omega + \frac{A_k}{2} V_{k'k}(\omega), \tag{B2}$$

$$\left(\omega + \Omega_0 - \frac{A_k + A_{k'}}{2}\right)\langle\langle I_k^- S^+ I_{k'}^-; S^+\rangle\rangle_\omega = \frac{A_k}{2}\langle\langle n_k I_{k'}^-; S^+\rangle\rangle_\omega + \frac{A_{k'}}{2}\langle\langle I_k^- n_{k'}; S^+\rangle\rangle_\omega - \frac{A_k}{2}\left\langle\left\langle I_{k'}^-\left(\frac{1}{2} - S^z\right); S^+\right\rangle\right\rangle_\omega - \frac{A_{k'}}{2}\left\langle\left\langle I_k^-\left(\frac{1}{2} - S^z\right); S^+\right\rangle\right\rangle_\omega + \sum_{k''(k,k')} \frac{A_{k''}}{2}\langle\langle I_k^- I_{k''}^+ I_{k'}^-; S^+\rangle\rangle_\omega, \tag{B3}$$

$$\left(\omega - \Omega_0 + \frac{A_k + A_{k'}}{2}\right)\langle\langle I_k^- I_{k'}^+ S^-; S^+\rangle\rangle_\omega = \frac{A_{k'}}{2}\left\langle\left\langle I_k^-\left(\frac{1}{2} - S^z\right); S^+\right\rangle\right\rangle_\omega - \frac{A_{k'}}{2}\langle\langle I_k^- n_{k'}; S^+\rangle\rangle_\omega - \sum_{k''(k,k')} \frac{A_{k''}}{2}\langle\langle I_k^- I_{k'}^+ I_{k''}^-; S^+\rangle\rangle_\omega, \tag{B4}$$

$$\left(\omega - \frac{A_k + A_{k''} - A_{k'}}{2}\right)\langle\langle I_k^- I_{k'}^+ I_{k''}^-; S^+\rangle\rangle_\omega = -\frac{A_k}{2}\langle\langle I_{k''}^- I_{k'}^+ S^-; S^+\rangle\rangle_\omega + \frac{A_{k'}}{2}\langle\langle I_k^- S^+ I_{k''}^-; S^+\rangle\rangle_\omega - \frac{A_{k''}}{2}\langle\langle I_k^- I_{k'}^+ S^-; S^+\rangle\rangle_\omega. \tag{B5}$$

These equations, together with Eq. (10), form a closed set. In

Sec. III, we find approximate solutions in the low-frequency ($\omega \sim 1$) and high-frequency ($\omega \sim \Omega$) regions separately.

APPENDIX C: EVALUATION OF $\sigma_n(\omega)$

Here we calculate the real and imaginary parts of $\sigma_n(\omega)$ [defined in Eq. (41)] in the low-energy solution of partially polarized and unpolarized nuclei in Sec. III. The spectral function of the electron-spin correlation function calculated from $\sigma_n(\omega)$ is then used to obtain the renormalized spin precession frequency and decay of electron-spin coherence.

There are three steps in the calculation of $\sigma_n(\omega)$. First we perform analytical continuation by replacing ω with $\omega + i0^+$ to obtain the retarded expressions. We then use the relation $\frac{1}{x+i0^+} = P\frac{1}{x} - i\pi\delta(x)$ to separate the principle values and the imaginary parts. Finally we evaluate the sum over the nuclear sites k by converting it into an integral, $\Sigma_k \to \int_0^\infty dk$. The validity and efficiency of this conversion have been discussed before.[22] Recall that $\sigma_2(\omega)$ is defined as

$$\sigma_2(\omega) = \sum_k \frac{A_k}{\omega - \frac{A_k}{2}} - \sum_k \frac{A_k}{\omega + \frac{A_k}{2}}. \tag{C1}$$

Using the procedures described above we find that the real and imaginary parts of $\sigma_2(\omega)$ are

$$\mathrm{Re}\ \sigma_2(\omega) = -2N\left[\ln\left|1 + \frac{1}{2\omega}\right| + \ln\left|1 - \frac{1}{2\omega}\right|\right], \tag{C2}$$

and

$$\mathrm{Im}\ \sigma_2(\omega) = \begin{cases} -2N\pi & 0 < \omega < \frac{1}{2} \\ 2N\pi & -\frac{1}{2} < \omega < 0. \end{cases} \tag{C3}$$

$\sigma_3(\omega)$ and $\sigma_4(\omega)$ can be evaluated in a similar manner. We obtain

$$\mathrm{Re}\ \sigma_3(\omega) = -4N + 4N\omega \ln\left|\frac{2\omega+1}{2\omega-1}\right|, \tag{C4}$$

$$\mathrm{Im}\ \sigma_3(\omega) = -4N\pi\omega, \quad -\frac{1}{2} < \omega < \frac{1}{2}, \tag{C5}$$

$$\mathrm{Re}\ \sigma_4(\omega) = -2N - 8N\omega^2\left[\ln\left|1 + \frac{1}{2\omega}\right| + \ln\left|1 - \frac{1}{2\omega}\right|\right], \tag{C6}$$

$$\mathrm{Im}\ \sigma_4(\omega) = \begin{cases} -8N\pi\omega^2 & 0 < \omega < \frac{1}{2} \\ 8N\pi\omega^2 & -\frac{1}{2} < \omega < 0. \end{cases} \tag{C7}$$

The imaginary parts of σ_n vanish beyond the regions listed above. Both $\omega = \pm\frac{1}{2}$ and $\omega = 0$ are branch points for σ_n. The two branch cuts ($[-1/2, 0]$ and $[0, 1/2]$) come from different dynamical fields of the electron felt by the nucleus, i.e., $\frac{A_k}{4}$ when $S^z = \frac{1}{2}$, and $-\frac{A_k}{4}$ when $S^z = -\frac{1}{2}$. In contrast only $\omega = -\frac{1}{2}$ appears as a branch point in the fully polarized case because $S^z = 1/2$ ($n_d = 0$) makes no contribution to the Hamiltonian in Eq. (A2).

APPENDIX D: EVALUATION OF SELF-ENERGY TERMS $\Sigma_1(\tilde{\omega})$, $\Sigma_2(\tilde{\omega})$, AND $\Sigma_3(\tilde{\omega})$ FOR PARTIALLY POLARIZED OR UNPOLARIZED NUCLEAR RESERVOIRS

Using the definitions of the self-energy terms given in Eqs. (54)–(56), we obtain analytical expressions of the real and imaginary parts of these self-energy terms. The same procedures as we have described in Appendix C are used in the following calculations. We first express Σ_1 as a two-dimensional integral:

$$\Sigma_1(\tilde{\omega}) = \sum_{k,k'} \frac{A_k^2 A_{k'}^2}{\tilde{\omega} + \frac{A_k - A_{k'}}{2}} = N^2 \int_0^1 dx \int_0^1 dy \frac{xy}{\tilde{\omega} + \frac{x-y}{2}}, \tag{D1}$$

where we have written A_k and $A_{k'}$ as integral variables x and y. The two-dimensional integral can be calculated, so that

$$\mathrm{Re}\ \Sigma_1(\tilde{\omega}) = -\frac{2N^2}{3}\left[\tilde{\omega} + 4\tilde{\omega}^3 \ln\left|1 - \frac{1}{4\tilde{\omega}^2}\right| - 3\tilde{\omega}\ln\left|1 - \frac{1}{4\tilde{\omega}^2}\right| + \ln\left|\frac{2\tilde{\omega}-1}{2\tilde{\omega}+1}\right|\right], \tag{D2}$$

$$\mathrm{Im}\ \Sigma_1(\tilde{\omega}) = -\frac{2N^2}{3}[4|\tilde{\omega}|^3 - 3|\tilde{\omega}| + 1]. \tag{D3}$$

The imaginary part of $\Sigma_1(\tilde{\omega})$ is nonvanishing only when $-\frac{1}{2} < \tilde{\omega} < \frac{1}{2}$. Similarly,

$$\Sigma_2(\tilde{\omega}) = N^3 \int_0^1 dx \int_0^1 dy \int_0^1 dz \frac{xyz}{\left(\tilde{\omega} + \frac{x-y}{2}\right)\left(\tilde{\omega} + \frac{x-z}{2}\right)}. \tag{D4}$$

$$\mathrm{Re}\ \Sigma_2(\tilde{\omega}) = 4N^3 \int_0^1 ds\ s\left[1 + (2\omega + s)\ln\left|\frac{2\tilde{\omega}+s-1}{2\tilde{\omega}+s}\right|\right],$$

$$\text{Im}\,\Sigma_2(\tilde{\omega}) = \begin{cases} \dfrac{1}{2} - \ln|1-2\tilde{\omega}| - 2\tilde{\omega} + \dfrac{8\tilde{\omega}}{3}\ln|1-2\tilde{\omega}| + \dfrac{10\tilde{\omega}^2}{3} - \dfrac{8\tilde{\omega}^3}{3} - \dfrac{16\tilde{\omega}^4}{3}\ln\left|\dfrac{1}{2\tilde{\omega}} - 1\right|, & 0 < \tilde{\omega} < \dfrac{1}{2} \\ \dfrac{1}{2} - 2\tilde{\omega} - 8\tilde{\omega}\ln|1-2\tilde{\omega}| + \dfrac{16\tilde{\omega}^2}{3}\ln|1+2\tilde{\omega}| + 8\tilde{\omega}^2\ln\left|\dfrac{1}{2\tilde{\omega}} + 1\right| - \dfrac{14\tilde{\omega}^2}{3} + \dfrac{8\tilde{\omega}^3}{3} - \dfrac{16\tilde{\omega}^4}{3}\ln\left|\dfrac{1}{2\tilde{\omega}} + 1\right|, & -\dfrac{1}{2} < \tilde{\omega} < 0. \end{cases} \tag{D5}$$

Repeating the calculation for $\Sigma_3(\tilde{\omega})$, we find that $\Sigma_3(\tilde{\omega})=\Sigma_2(\tilde{\omega})$. The integral in Eq. (D5) can be computed numerically. However, the calculation is nontrivial because of the singularities appearing in the expression. Alternatively, the integral can be done analytically using MAPLE. The result, which is too complicated to be presented here, is a sum of terms that include the dilog functions defined as $f_{\text{dilog}}(x)=\int_0^x \ln t/(1-t)dt$.[61] Numerical calculation of the real part of $\Sigma_2(\tilde{\omega})$ using the analytical expression obtained with MAPLE is very accurate when we check the sum rule of the spectrum function numerically (see discussions in Sec. III).

[1] T. Fujisawa, D. G. Austing, Y. Tokura, Y. Hirayama, and S. Tarucha, Nature (London) **419**, 278 (2002).
[2] K. Ono, D. G. Austing, Y. Tokura, and S. Tarucha, Science **297**, 1313 (2002).
[3] M. Kroutvar, Y. Ducommun, D. Heiss, M. Bichler, D. Schuh, G. Abstreiter, and J. J. Finley, Nature (London) **432**, 81 (2004).
[4] J. R. Petta, A. C. Johnson, J. M. Taylor, E. A. Laird, A. Yacoby, M. D. Lukin, C. M. Marcus, M. P. Hanson, and A. C. Gossard, Science **309**, 2180 (2005).
[5] F. H. L. Koppens, J. A. Folk, J. M. Elzerman, R. Hanson, L. H. Willems van Beveren, I. T. Vink, H. P. Tranitz, W. Wegscheider, L. P. Kouwenhoven, and L. M. K. Vandersypen, Science **309**, 1346 (2005).
[6] T. Hatano, M. Stopa, and S. Tarucha, Science **309**, 268 (2005).
[7] F. H. L. Koppens, C. Buizert, K. J. Tielrooij, I. T. Vink, K. C. Nowack, T. Meunier, L. P. Kouwenhoven, and L. M. K. Vandersypen, Nature (London) **442**, 766 (2006).
[8] H. J. Krenner, E. C. Clark, T. Nakaoka, M. Bichler, C. Scheurer, G. Abstreiter, and J. J. Finley, Phys. Rev. Lett. **97**, 076403 (2006).
[9] A. Greilich, D. R. Yakovlev, A. Shabaev, Al. L. Efros, I. A. Yugova, R. Oulton, V. Stavarache, D. Reuter, A. Wieck, and M. Bayer, Science **313**, 341 (2006).
[10] R. Oulton, A. Greilich, S. Y. Verbin, R. V. Cherbunin, T. Auer, D. R. Yakovlev, M. Bayer, I. A. Merkulov, V. Stavarache, D. Reuter, and A. D. Wieck, Phys. Rev. Lett. **98**, 107401 (2007).
[11] K. C. Nowack, F. H. L. Koppens, Yu. V. Nazarov, and L. M. K. Vandersypen, Science **318**, 1430 (2007).
[12] F. H. L. Koppens, K. C. Nowack, and L. M. K. Vandersypen, Phys. Rev. Lett. **100**, 236802 (2008).
[13] D. J. Reilly, J. M. Taylor, J. R. Petta, C. M. Marcus, M. P. Hanson, and A. C. Gossard, Science **321**, 817 (2008).
[14] R. Hanson, L. P. Kouwenhoven, J. R. Petta, S. Tarucha, and L. M. K. Vandersypen, Rev. Mod. Phys. **79**, 1217 (2007).
[15] G. Burkard, D. Loss, and D. P. DiVincenzo, Phys. Rev. B **59**, 2070 (1999).
[16] X. Hu and S. Das Sarma, Phys. Rev. A **61**, 062301 (2000).
[17] I. A. Merkulov, A. L. Efros, and M. Rosen, Phys. Rev. B **65**, 205309 (2002).
[18] J. Schliemann, A. V. Khaetskii, and D. Loss, Phys. Rev. B **66**, 245303 (2002).
[19] A. V. Khaetskii, D. Loss, and L. Glazman, Phys. Rev. Lett. **88**, 186802 (2002); Phys. Rev. B **67**, 195329 (2003).
[20] R. de Sousa and S. Das Sarma, Phys. Rev. B **67**, 033301 (2003); **68**, 115322 (2003).
[21] V. N. Golovach, A. Khaetskii, and D. Loss, Phys. Rev. Lett. **93**, 016601 (2004).
[22] W. A. Coish and D. Loss, Phys. Rev. B **70**, 195340 (2004).
[23] S. I. Erlingsson and Y. V. Nazarov, Phys. Rev. B **70**, 205327 (2004).
[24] N. Shenvi, R. de Sousa, and K. B. Whaley, Phys. Rev. B **71**, 224411 (2005).
[25] W. M. Witzel, R. deSousa, and S. Das Sarma, Phys. Rev. B **72**, 161306(R) (2005).
[26] J. M. Taylor, H. A. Engel, W. Dur, A. Yacoby, C. M. Marcus, P. Zoller, and M. D. Lukin, Nat. Phys. **1**, 177 (2005).
[27] C. Deng and X. Hu, Phys. Rev. B **73**, 241303(R) (2006); **74**, 129902(E) (2006).
[28] W. Yao, R. B. Liu, and L. J. Sham, Phys. Rev. B **74**, 195301 (2006).
[29] W. M. Witzel and S. Das Sarma, Phys. Rev. B **74**, 035322 (2006); Phys. Rev. Lett. **98**, 077601 (2007).
[30] K. A. Al-Hassanieh, V. V. Dobrovitski, E. Dagotto, and B. N. Harmon, Phys. Rev. Lett. **97**, 037204 (2006).
[31] P. Stano and J. Fabian, Phys. Rev. Lett. **96**, 186602 (2006).
[32] W. Yao, R. B. Liu, and L. J. Sham, Phys. Rev. Lett. **98**, 077602 (2007); **98**, 099901 (2007).
[33] S. K. Saikin, W. Yao, and L. J. Sham, Phys. Rev. B **75**, 125314 (2007).
[34] W. M. Witzel, X. Hu, and S. Das Sarma, Phys. Rev. B **76**, 035212 (2007).
[35] R. Liu, W. Yao, and L. J. Sham, New J. Phys. **9**, 226 (2007).
[36] W. Yang and R. B. Liu, Phys. Rev. B **78**, 085315 (2008).
[37] D. Loss and D. P. DiVincenzo, Phys. Rev. A **57**, 120 (1998).
[38] X. Hu and S. Das Sarma, Phys. Status Solidi B **238**, 360 (2003); X. Hu, in *Quantum Coherence*, Lecture Notes in Physics Vol. 689, edited by W. Potz, J. Fabian, and U. Hohenester (Springer, Berlin, 2006), pp. 83–114; S. Das Sarma, R. de Sousa, X. Hu, and B. Koiller, Solid State Commun. **133**, 737 (2005).
[39] J. M. Taylor, C. M. Marcus, and M. D. Lukin, Phys. Rev. Lett.

90, 206803 (2003); J. M. Taylor, A. Imamoglu, and M. D. Lukin, *ibid.* **91**, 246802 (2003).
[40] C. Deng and X. Hu, IEEE Trans. Nanotechnol. **4**, 35 (2005).
[41] U. Weiss, *Quantum Dissipative Systems* (World Scientific, Singapore, 2001).
[42] N. Bloembergen and T. J. Rowland, Phys. Rev. **97**, 1679 (1955).
[43] C. P. Slichter, *Principles of Magnetic Resonance* (Spinger-Verlag, Berlin, 1996).
[44] A. Abragam, *The Principles of Nuclear Magnetism* (Oxford University Press, London, 1961).
[45] D. Paget, G. Lampel, B. Sapoval, and V. I. Safarov, Phys. Rev. B **15**, 5780 (1977).
[46] G. D. Mahan, *Many-Particle Physics* (Plenum, New York, 1990).
[47] P. W. Anderson, Phys. Rev. **124**, 41 (1961).
[48] C. M. Bender and S. A. Orszag, *Advanced Mathematical Methods for Scientists Engineers* (Spinger, New York, 1999).
[49] R. Winkler, *Spin-Orbit Coupling Effects in 2D Electron and Hole Systems* (Springer, Berlin, 2003), Appendix B.
[50] D. Gammon, E. S. Snow, B. V. Shanabrook, D. S. Katzer, and D. Park, Phys. Rev. Lett. **76**, 3005 (1996).
[51] K. Ono and S. Tarucha, Phys. Rev. Lett. **92**, 256803 (2004).
[52] J. Baugh, Y. Kitamura, K. Ono, and S. Tarucha, Phys. Rev. Lett. **99**, 096804 (2007).
[53] J. R. Petta, J. M. Taylor, A. C. Johnson, A. Yacoby, M. D. Lukin, C. M. Marcus, M. P. Hanson, and A. C. Gossard, Phys. Rev. Lett. **100**, 067601 (2008).
[54] At lower effective magnetic field it is foreseeable that multiple-pair flips within the nuclear-spin reservoir become more important and contribute significantly to the resulting electron-spin decoherence. Recent studies have pursued this problem using cluster expansion techniques (Refs. 29, 33, and 36).
[55] In general, T_2^* is the dephasing time in an inhomogeneously broadened (that is, with a distribution of frequencies) ensemble of spins, while T_2 represents spin coherence time after effects of inhomogeneous broadening are removed by means such as spin echoes. The coherence time calculated here is not a typical T_2 because we do not consider spin echo. Neither is it T_2^* because we consider single spin coherent properties. There is no ensemble of spins with different frequencies. Therefore, we give a new name T_2' to the coherence time we calculate here, which is a single spin property.
[56] C. Deng and X. Hu, Phys. Rev. B **71**, 033307 (2005).
[57] A. Imamo$\bar{\text{g}}$lu, E. Knill, L. Tian, and P. Zoller, Phys. Rev. Lett. **91**, 017402 (2003).
[58] C. W. Lai, P. Maletinsky, A. Badolato, and A. Imamoglu, Phys. Rev. Lett. **96**, 167403 (2006).
[59] F. Meier and B. P. Zakharchenya, *Optical Orientation* (North-Holland, Amsterdam, 1984).
[60] T. Giamarchi, *Quantum Physics in One Dimension* (Clarendon, Oxford, 2004).
[61] M. Abramowitz and I. A. Stegun, *Handbook of Mathematical Functions with Forms, Graphs, and Mathematical Tables* (Dover Publications, New York, 1965).